STRUCTURAL SCIENCE
CRYSTAL ENGINEERING
MATERIALS

Volume 78 (2022)

Supporting information for article:

Investigation of crystal structures, energetics and isostructurality in halogen-substituted phosphoradimates

Avantika Hasija, Shubham Som and Deepak Chopra

S.1. Synthesis:

The unsubstituted compound and halogen substituted phosphoradimates have been synthesized by nucleophilic substitution reaction wherein the unsubstituted/halogen-substituted anilines and DMAP act as a nucleophile and base, respectively. In a round bottom flask, 15.0 ml of dry dichloromethane was added, to which aniline and DMAP were added in 1:1.2 equimolar ratio and the solution was stirred for half an hour at 0-5ºC on magnetic stirrer under inert atmosphere. Subsequent addition of phosphoryl chloride with stirring for 7-8 hours at room temperature yields the respective halogen substituted phosphoramidates. The completion of the reaction was monitored using thin-layer chromatography. The quenching of the reaction was carried out using 5% hydrochloric acid. It was dried using sodium sulfate and finally purified by column chromatography. The products have been characterized through NMR and further crystallized using a library of solvents [dichloromethane, toluene, chloroform, nitromethane, dioxane, hexane, heptane, DCM-hexane, methanol, ethanol, isopropanol, isooctane, carbon tetrachloride, propanol, benzene, acetone, acetonitrile, ethyl acetate,

diethyl ether, trifluoro toluene]. The single crystal X-ray diffraction data for all the respective compounds were collected and are tabulated in Table 1.

S.2. Characterization:

S.2.1. NMR:

^{1}H NMR Spectra of synthesised bulk product- unsubstituted and halogenated phosphoradimates.

The aromatic protons (10) of both -OPh groups are overlapped in the range of 7.1-7.4ppm in the spectra shown below. In addition to this, based on the deshielding effect of halogen, some of the vicinity protons are merged with these aromatic protons (of -OPh) as shown in case of 00, 2Cl, 2Br, 2I, 3F, 3Cl and 3Br. The -NH protons were seen to lie in the range of 5.5-6.9ppm in the spectra.

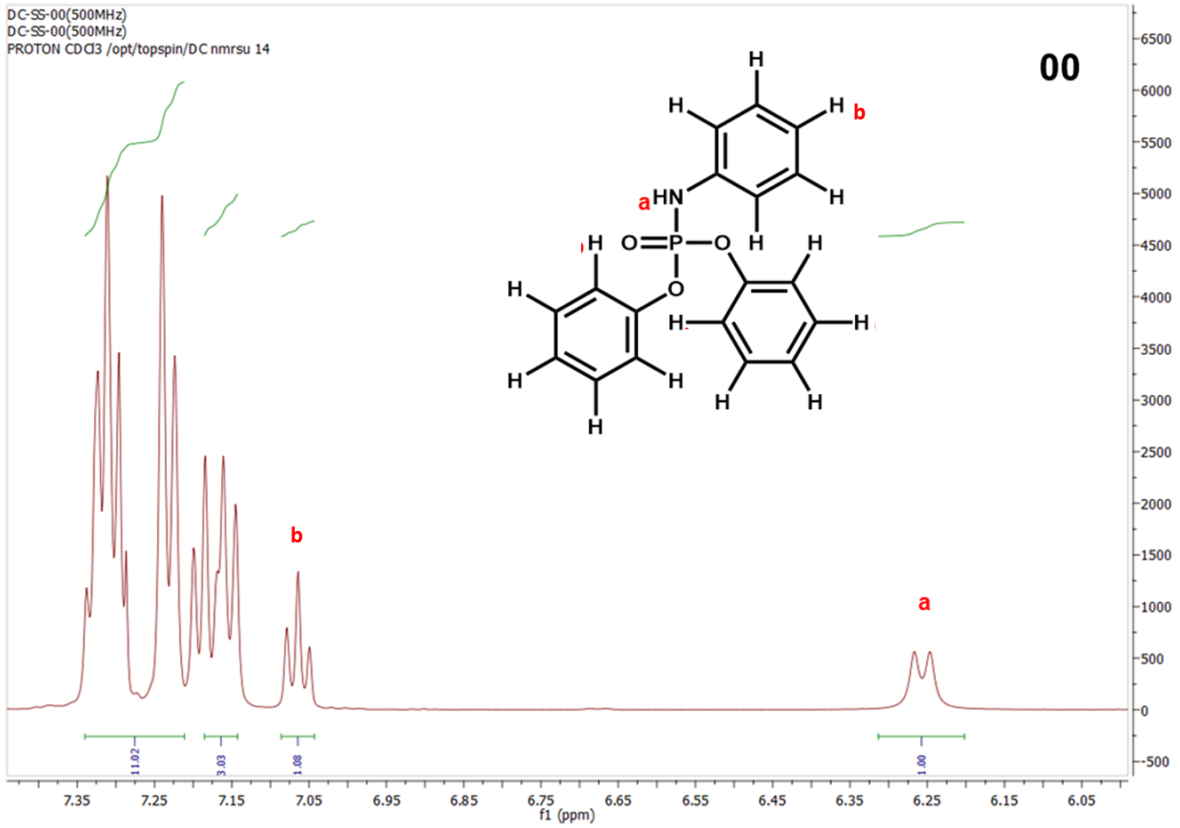
DC-SS-00(500MHz)
DC-SS-00(500MHz)
PROTON CDCl3 /opt/topspin/DC nmrsu 14
00
a
b
11.02
3.03
1.00
1.00
f1 (ppm)

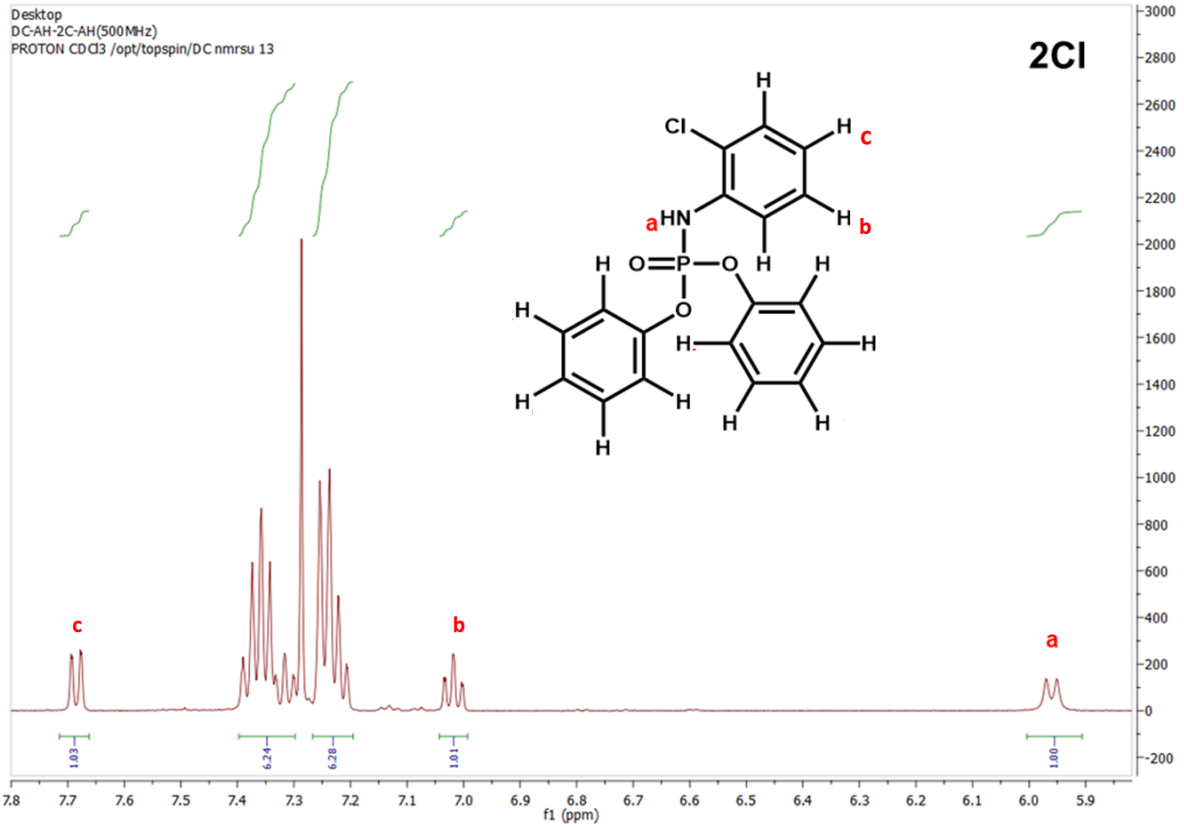
Desktop
DC-AH-2C-AH(500MHz)
PROTON CDCl3 /opt/topspin/DC nmrsu 13
2Cl
c
b
a
1.03
6.24
6.28
1.01
1.00
f1 (ppm)

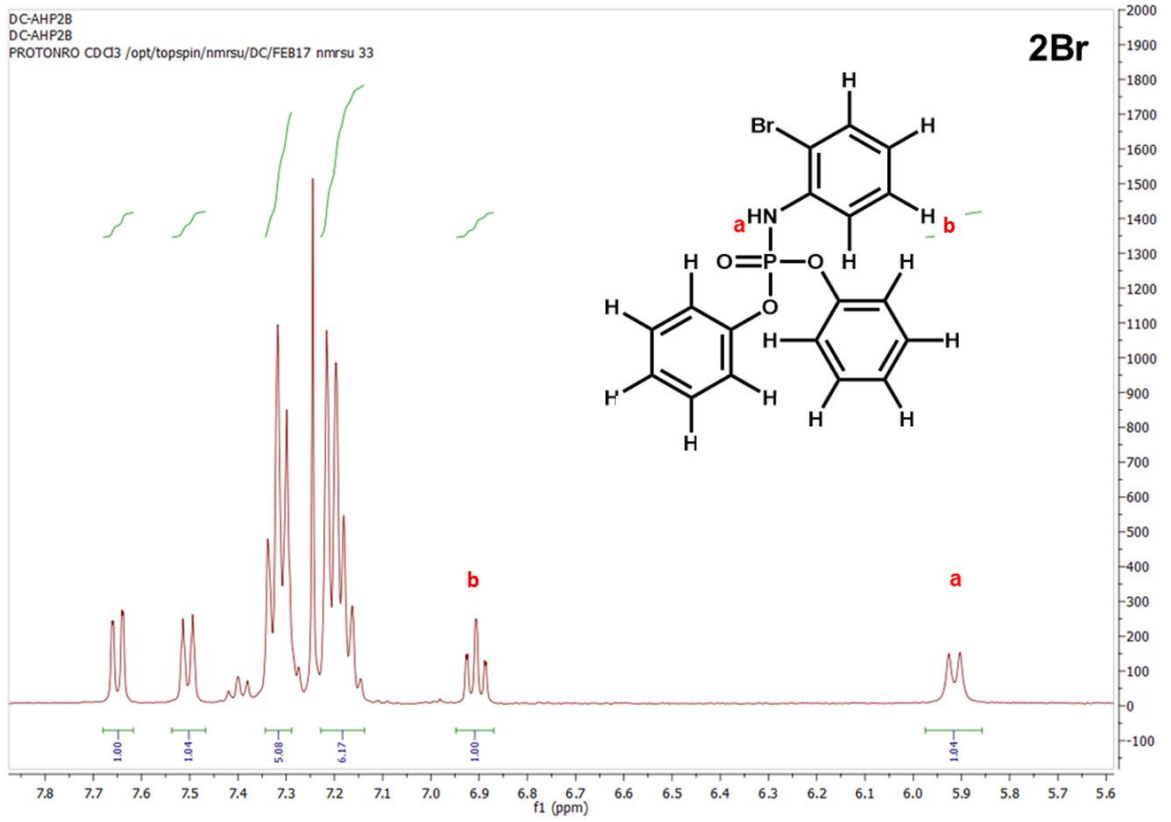
DC-AHP2B
DC-AHP2B
PROTONRO CDCl3 /opt/topspin/nmrsu/DC/FEB17 nmrsu 33
2Br
Br
a
b
f1 (ppm)

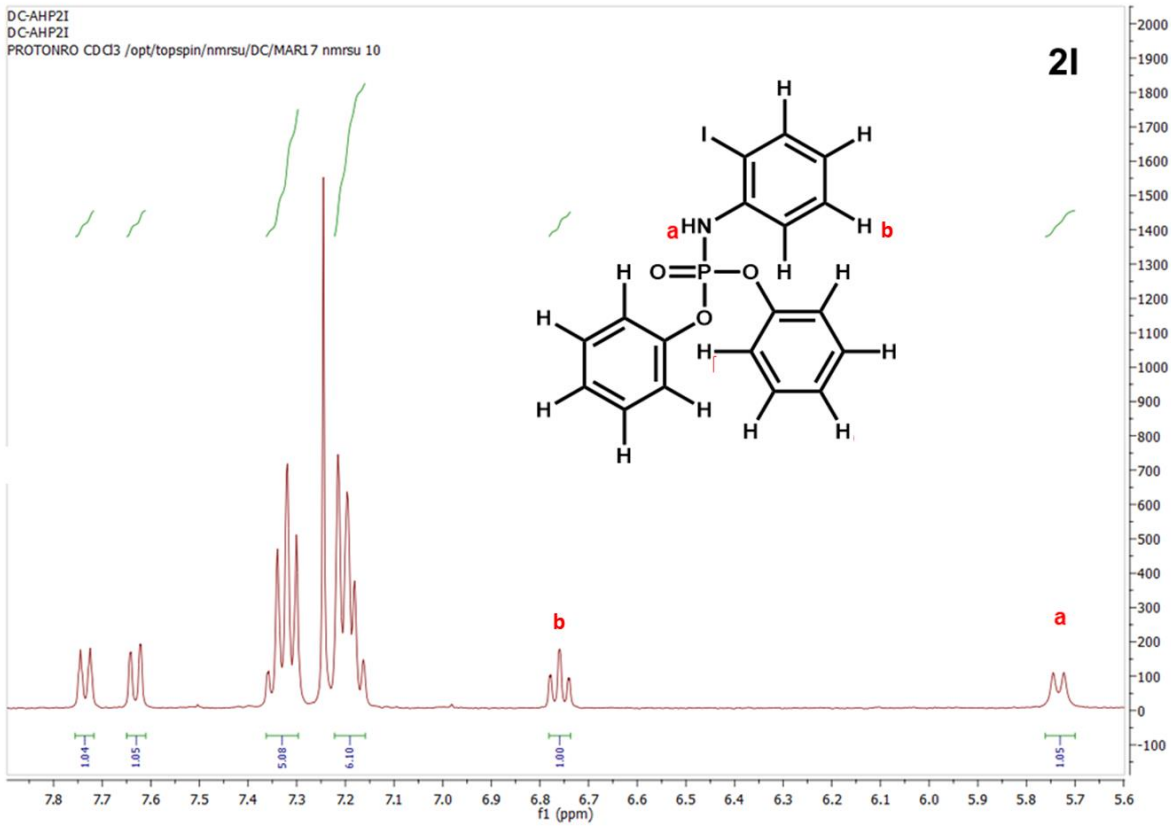
DC-AHP2I
DC-AHP2I
PROTONRO CDCl3 /opt/topspin/nmrsu/DC/MAR17 nmrsu 10
2I
I
a
b
f1 (ppm)

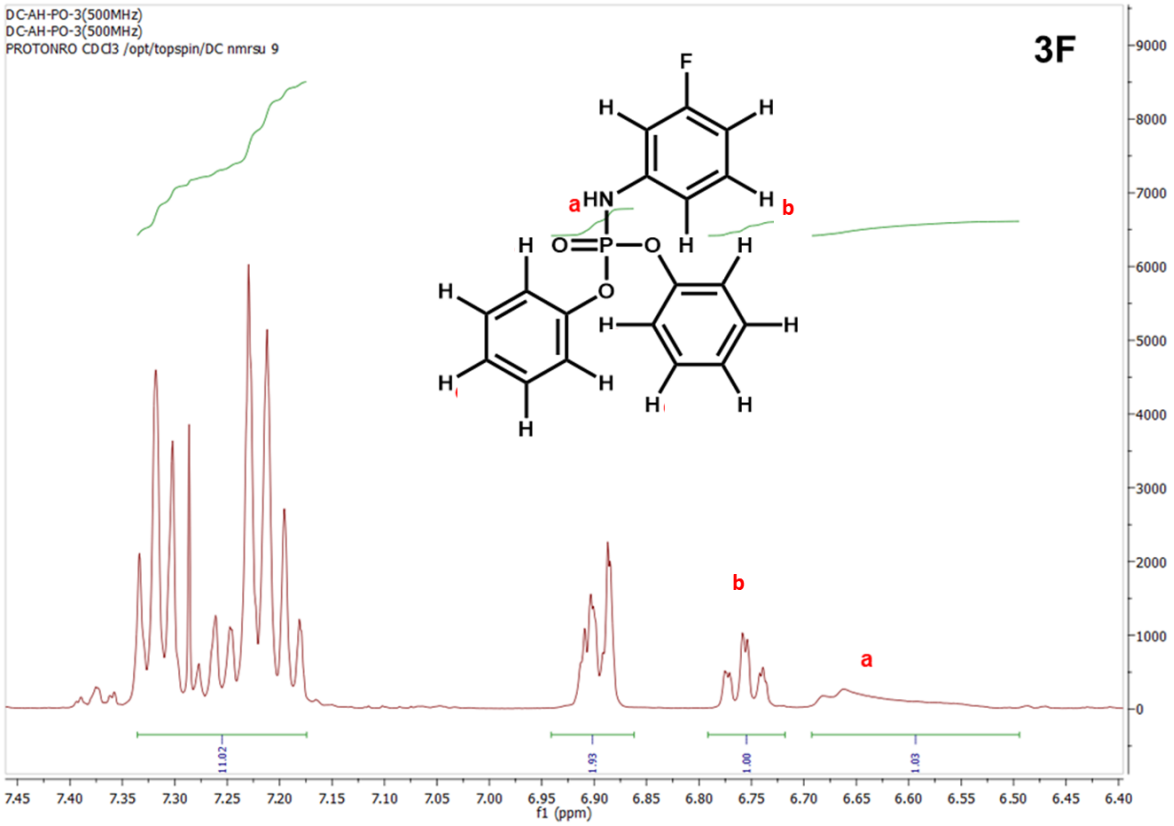
DC-AH-PO-3(500MHz)
DC-AH-PO-3(500MHz)
PROTONRO CDCl3 /opt/topspin/DC nmrsu 9
3F
F
H
HN
a
b
O=P—O
O
b
a
11.02
1.93
1.00
1.03
f1 (ppm)

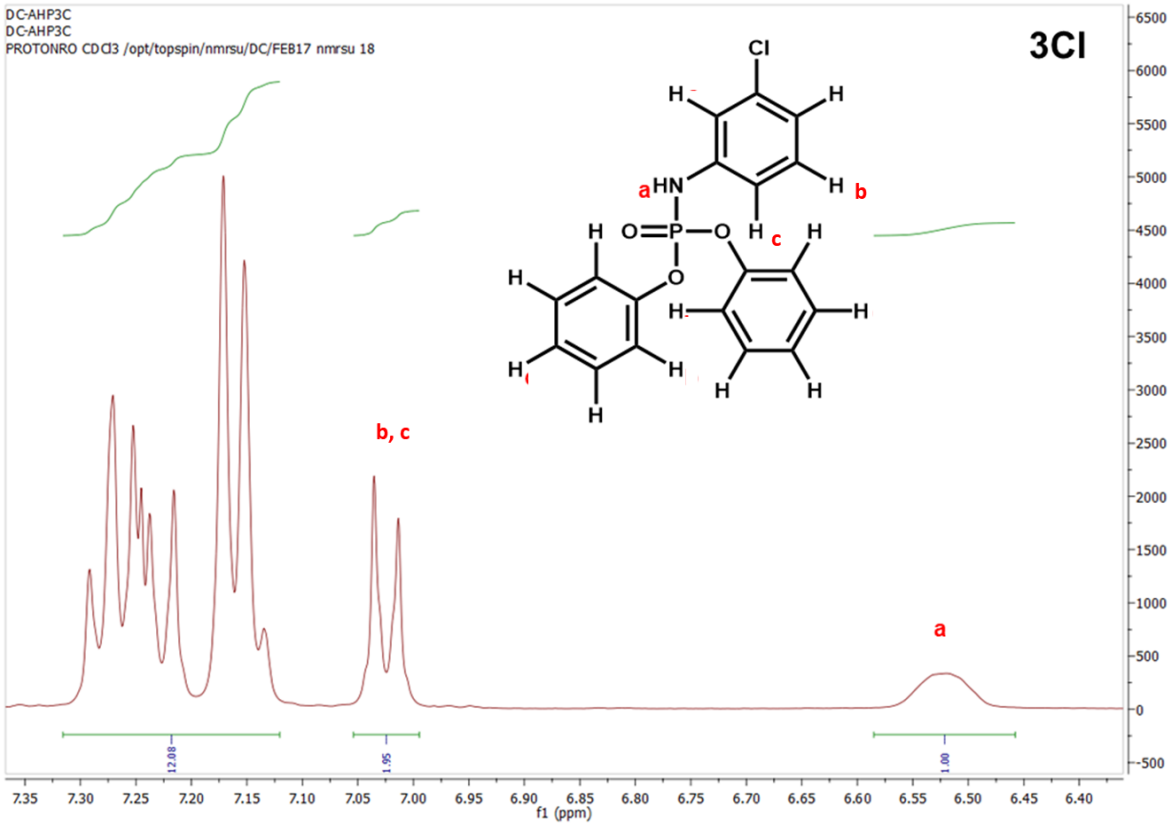
DC-AHP3C
DC-AHP3C
PROTONRO CDCl3 /opt/topspin/nmrsu/DC/FEB17 nmrsu 18
3Cl
Cl
H
HN
a
b
O=P—O
O
c
b, c
a
12.08
1.95
1.00
f1 (ppm)

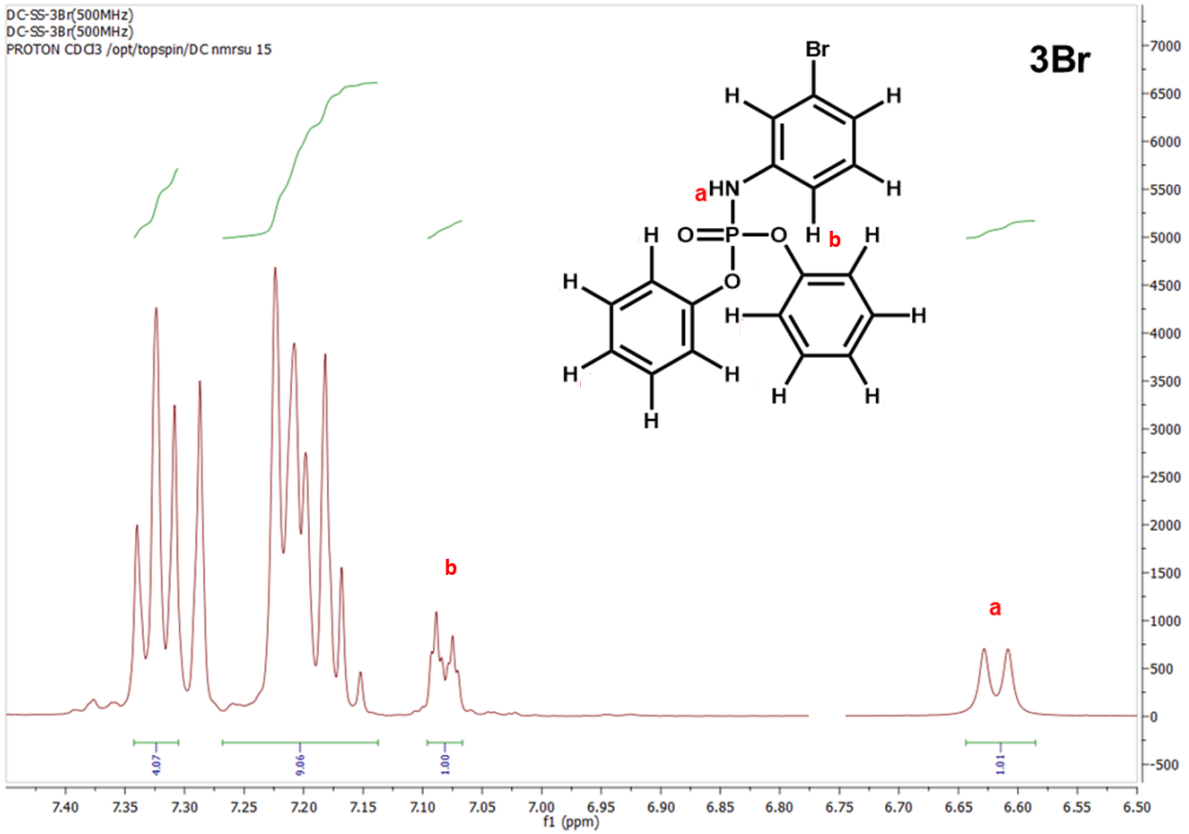
DC-SS-3Br(500MHz)
DC-SS-3Br(500MHz)
PROTON CDCl3 /opt/topspin/DC nmrsu 15
3Br
Br
a
b
4.07
9.06
1.00
1.01
f1 (ppm)

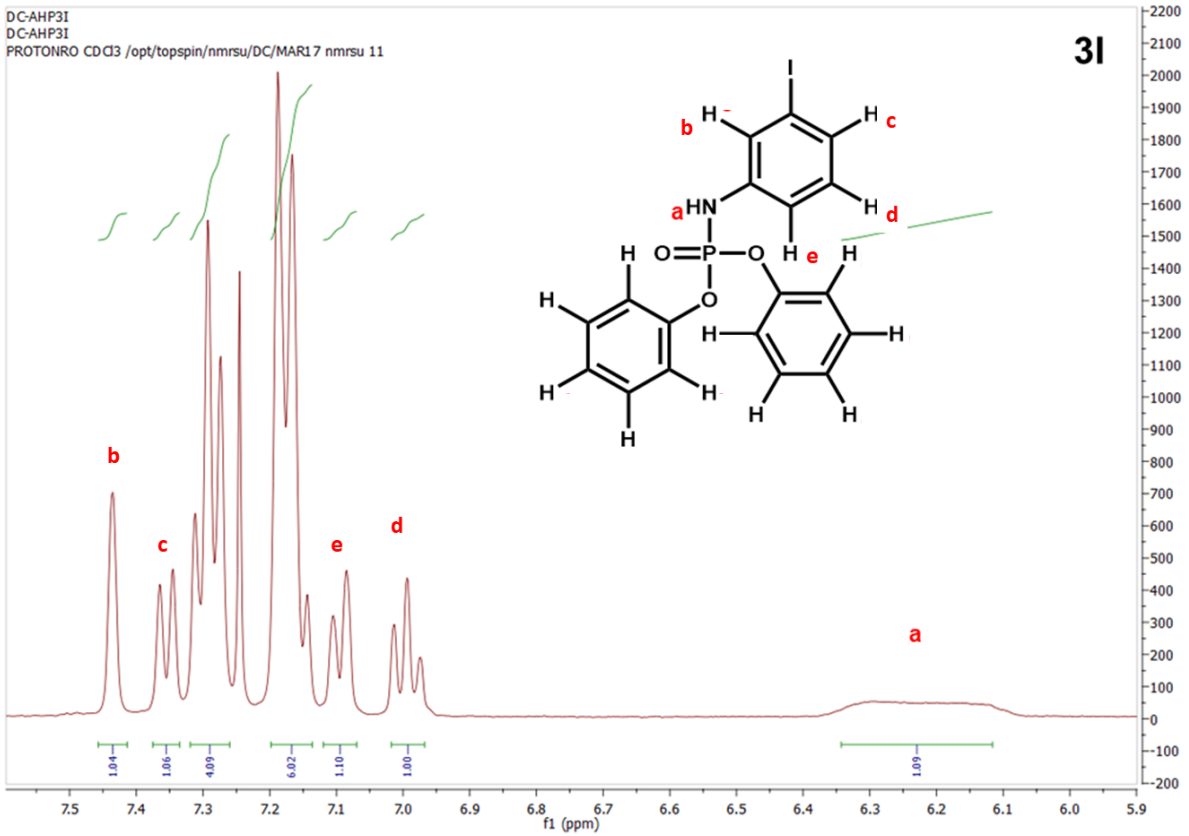
DC-AHP3I
DC-AHP3I
PROTONRO CDCl3 /opt/topspin/nmrsu/DC/MAR17 nmrsu 11
3I
I
a
b
c
d
e
1.04
1.06
4.09
6.02
1.10
1.00
1.09
f1 (ppm)

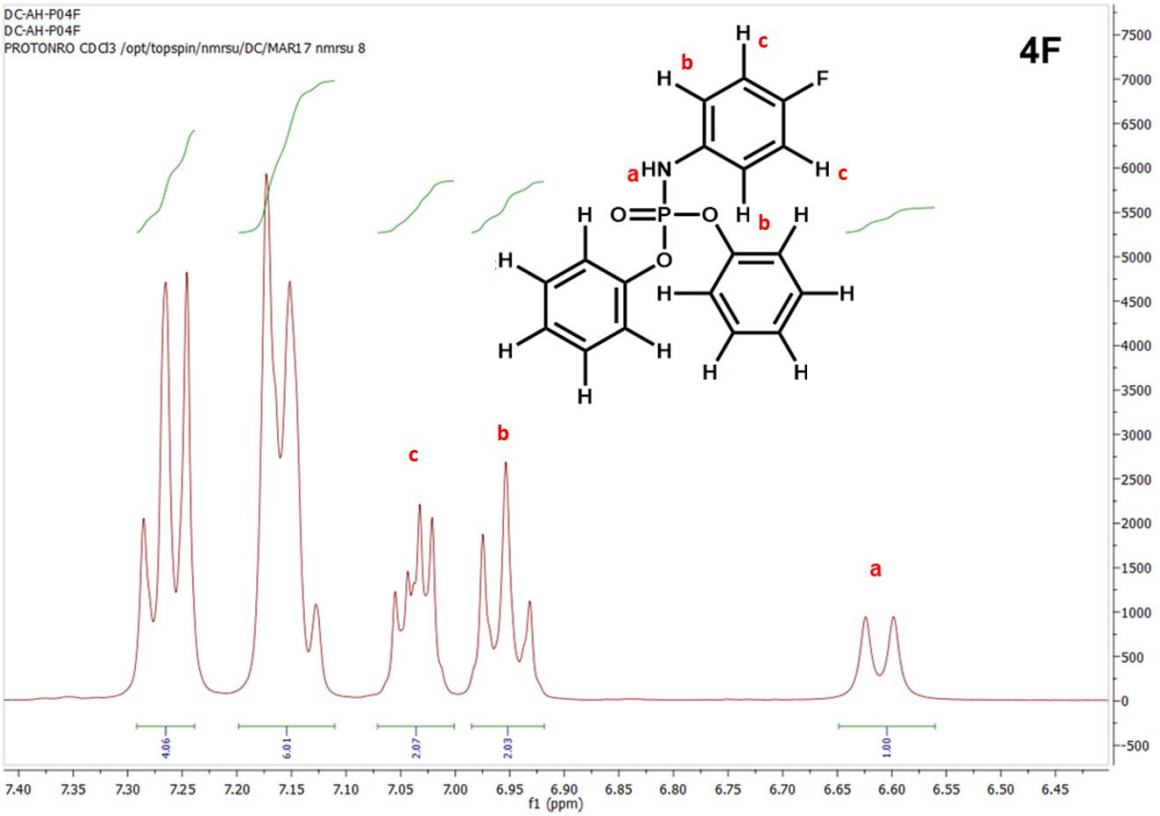
DC-AH-P04F
DC-AH-P04F
PROTONRO CDCl3 /opt/topspin/nmrsu/DC/MAR17 nmrsu 8
4F
a
b
c
4.06
6.01
2.07
2.03
1.00
f1 (ppm)

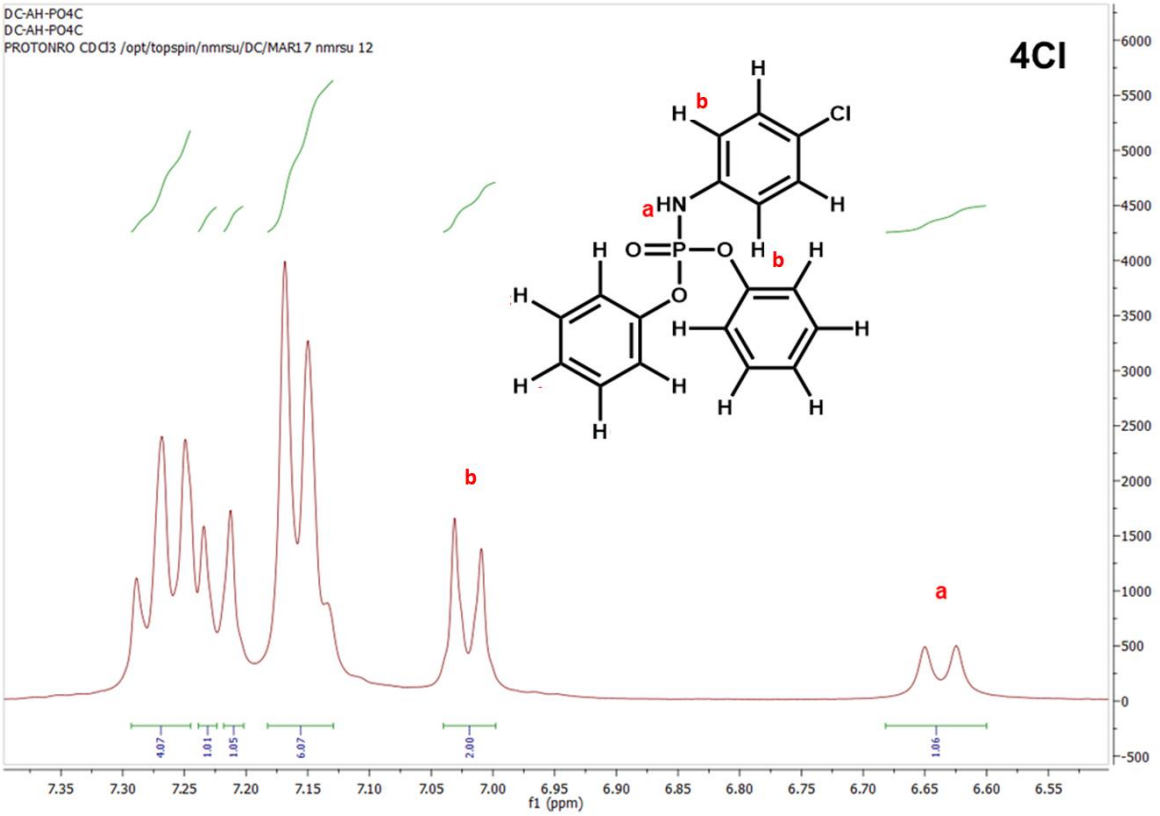
DC-AH-P04C
DC-AH-P04C
PROTONRO CDCl3 /opt/topspin/nmrsu/DC/MAR17 nmrsu 12
4Cl
a
b
4.07
1.01
1.05
6.07
2.00
1.06
f1 (ppm)

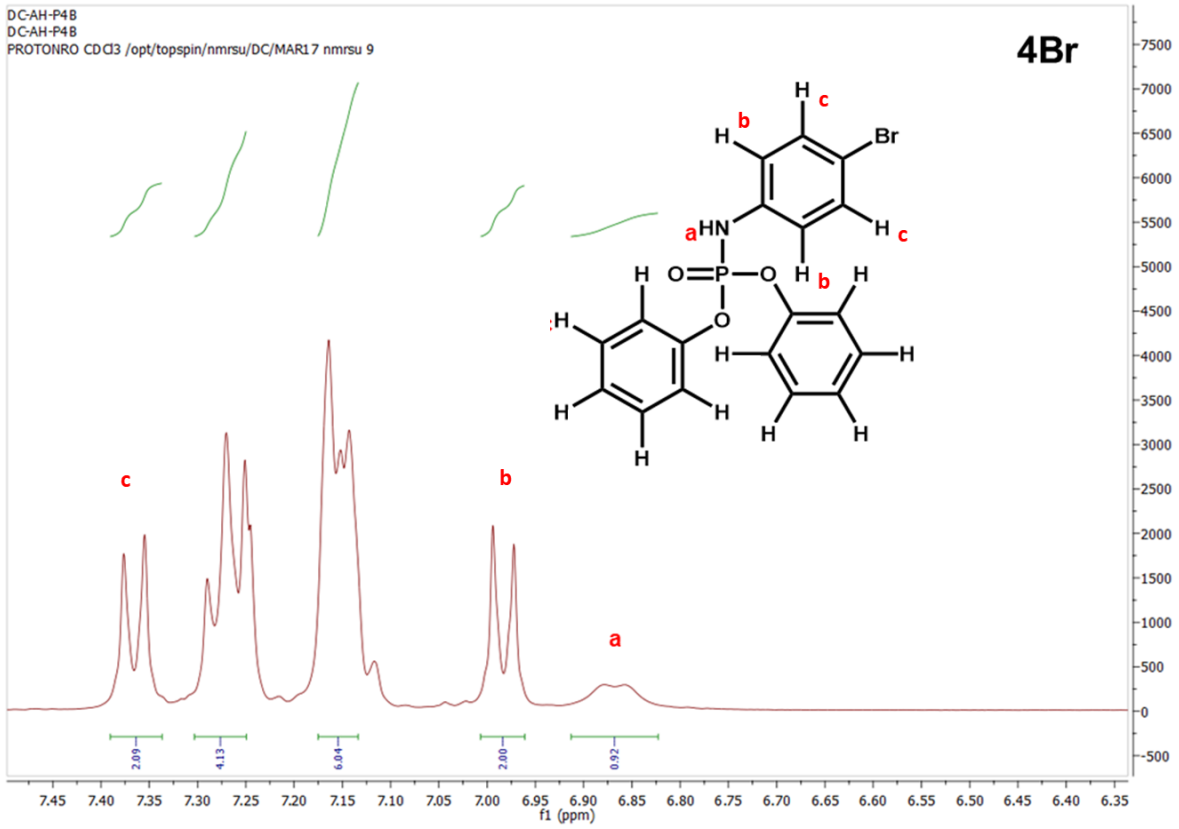
DC-AH-P4B
DC-AH-P4B
PROTONRO CDCl3 /opt/topspin/nmrsu/DC/MAR17 nmrsu 9
4Br
c
b
a
2.09
4.13
6.04
2.00
0.92
f1 (ppm)

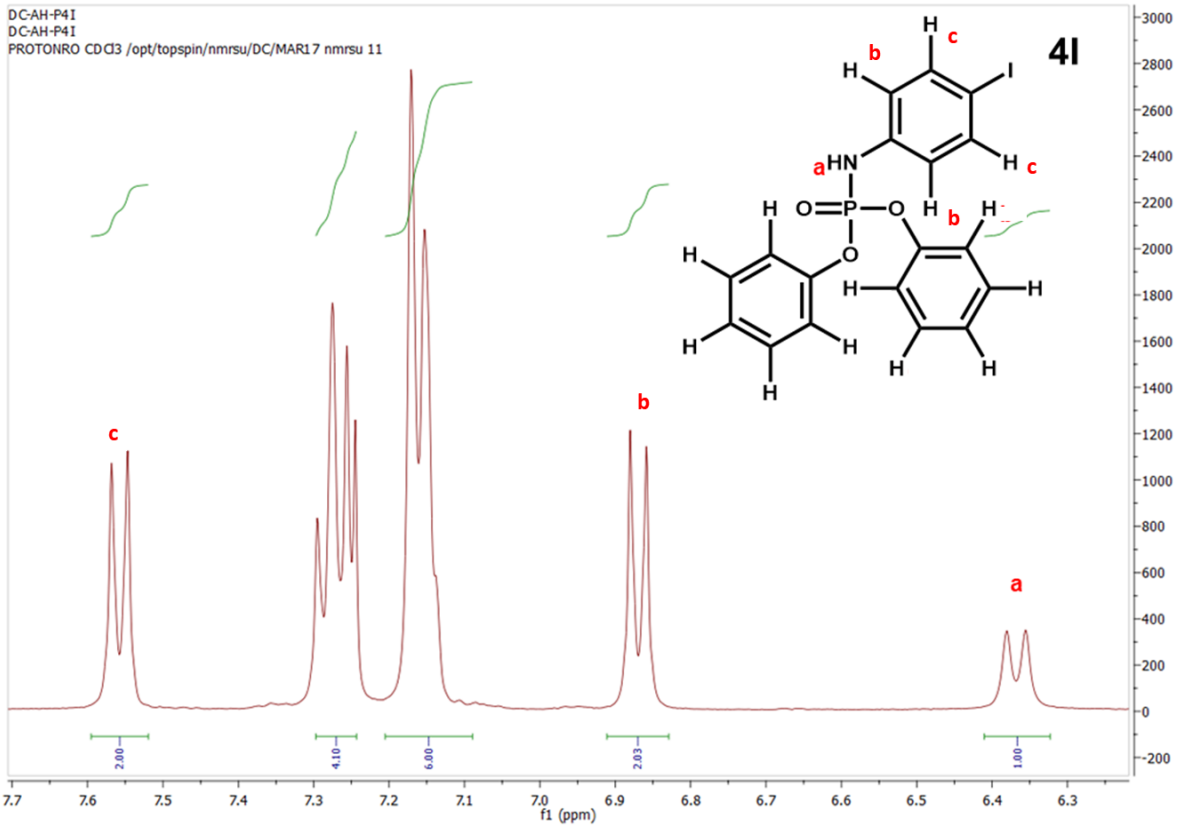
DC-AH-P4I
DC-AH-P4I
PROTONRO CDCl3 /opt/topspin/nmrsu/DC/MAR17 nmrsu 11
4I
c
b
a
2.00
4.10
6.00
2.03
1.00
f1 (ppm)

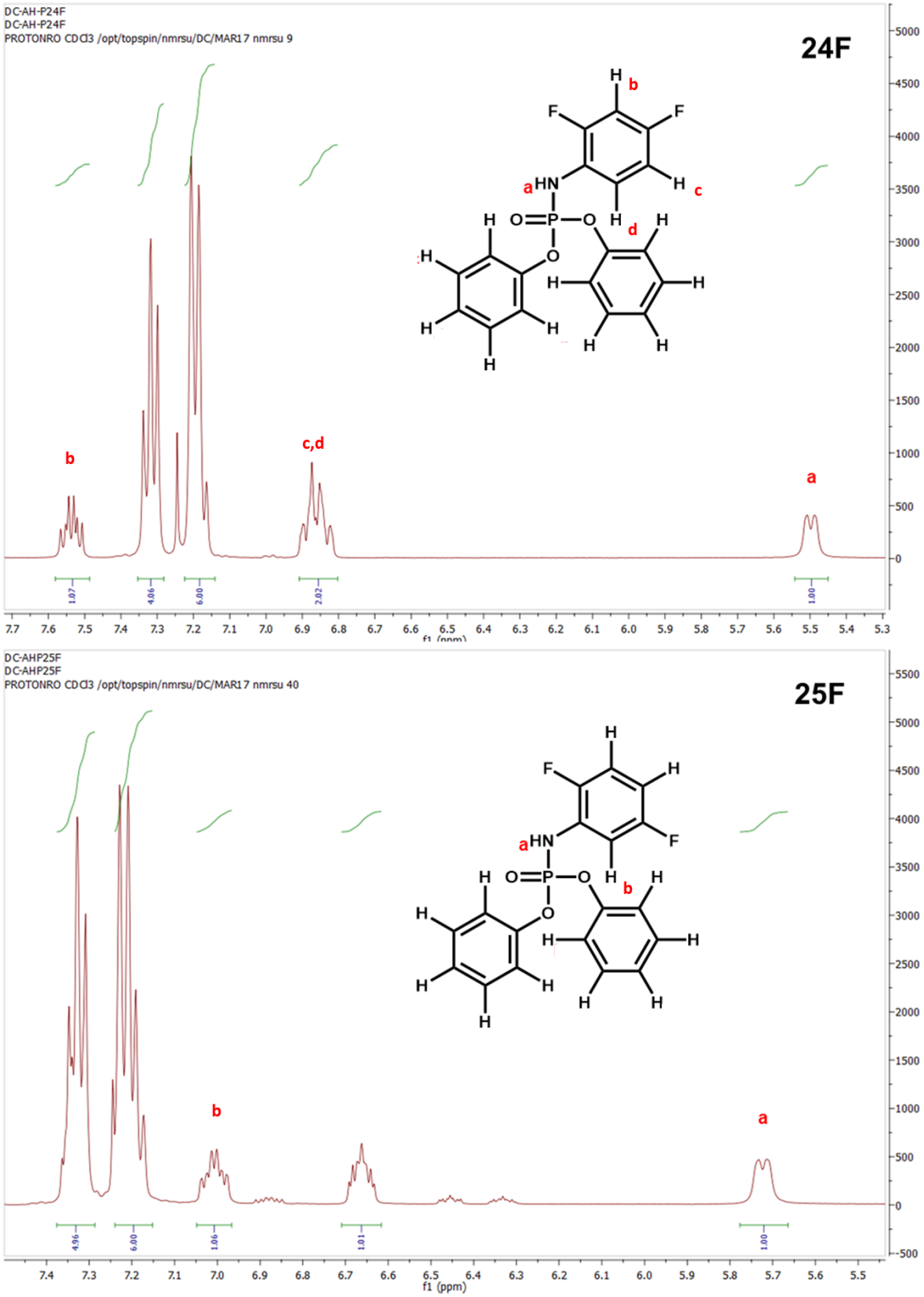

S.2.2. Thermal Characterization: Differential Scanning Calorimetry (DSC) traces for all the synthesised compounds were recorded with a PerkinElmer DSC 6000 instrument, in hermetically sealed

aluminium pan under vacuum and subsequently scanned at a rate of 5 °C/min under a dry nitrogen purge (20 mL/min).

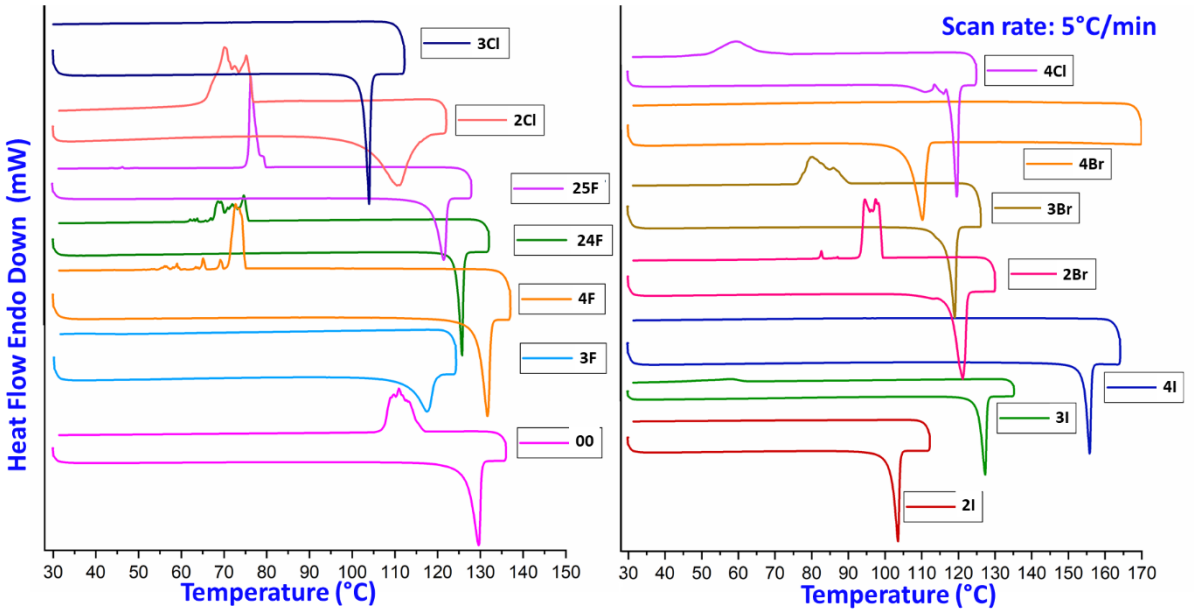

Fig S1: DSC traces for halogenated phosphoradimates recorded at a scan rate of 5°C/min.

Table S1: Melting Point of unsubstituted and halogenated phosphoradimates.

S. No.	Compound	Melting Point (°C)	S. No.	Compound	Melting Point (°C)
1.	00	129.6	**8.**	4Cl	119.0
2.	3F	117.2	**9.**	2Br	121.2
3.	4F	131.7	**10.**	3Br	119.0
4.	24F	125.8	**11.**	4Br	110.2
5.	25F	121.6	**12.**	2I	103.6
6.	2Cl	110.4	**13.**	3I	127.4
7.	3Cl	104.0	**14.**	4I	155.8

S.2.3. Powder X-ray diffraction (PXRD):

The experimental powder X-ray diffraction patterns of synthesized unsubstituted and halogenated phosphoradimates were recorded on a PANalytical Empyrean X-ray Diffractometer with Cu Kα radiation (λ = 1.5418 Å). The bulk powder of each sample was placed in a silica sample holder and measured by a continuous scan between 5 and 50° in 2θ with a step size of 0.013103°.

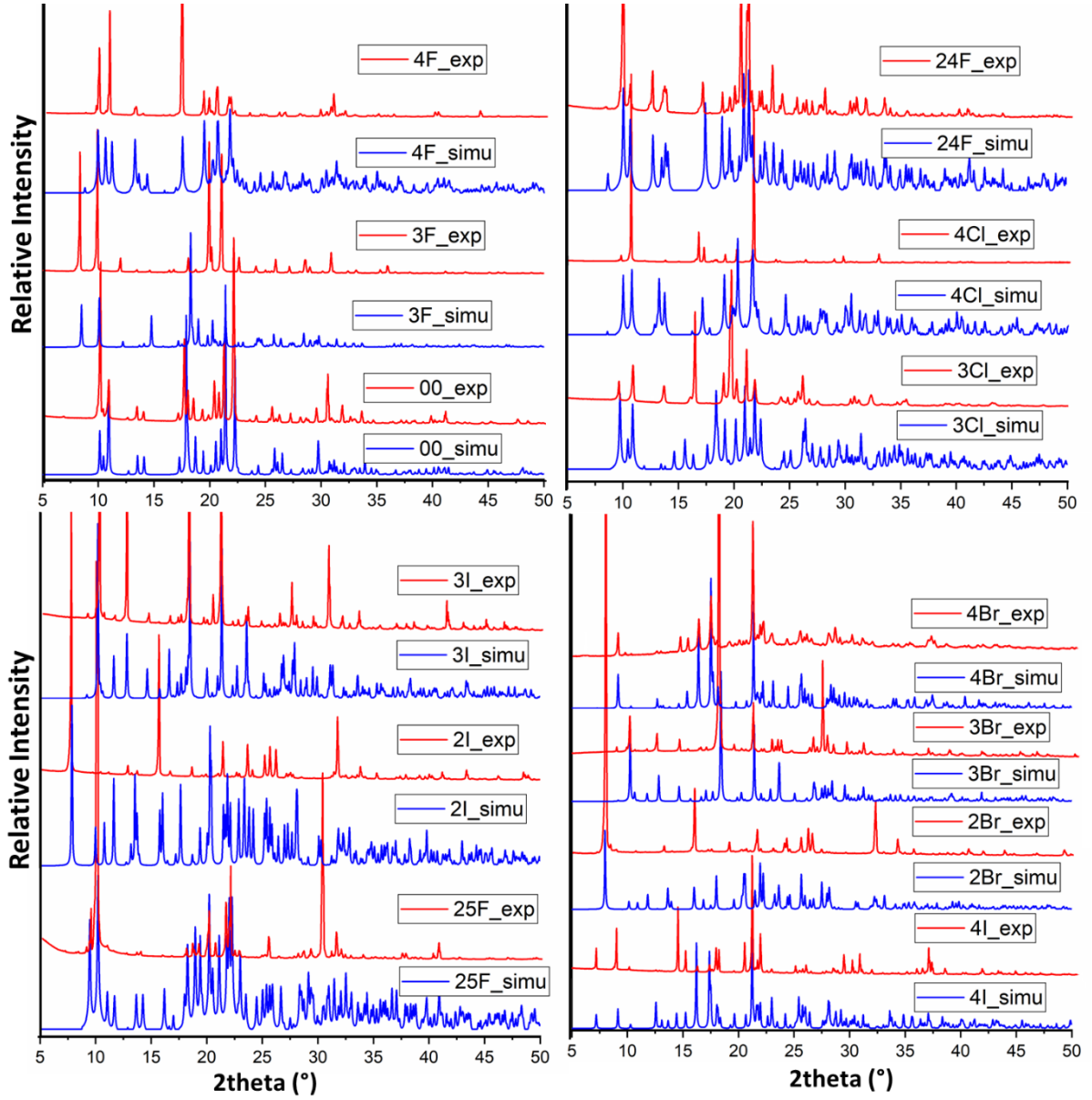

Fig S2: Overlay of experimental (red) and simulated (blue) powder profile for all synthesised phosphoradimates (X-axis represents 2theta (°); Y-axis represent relative intensity); Powder diffraction profiles of 2Br, 2I, 3Br, 4I and 00 have been submitted for inclusion in the Powder Diffraction Files (PDF)(Gates-Rector & Blanton, 2019) to the ICDD Grant-in-Aid Program under Grant ID: 20-07.

S.2.4. Single crystal X-ray diffraction (SCXRD):

Single-crystal X-ray diffraction data were collected on Bruker AXS Kappa APEX II diffractometer using Mo K_α radiation (λ = 0.71073 Å) and APEX II software [Bruker, 2006] at temperature 100(2) K, maintained using Oxford Cryostream low-temperature device. Data integration and reduction were carried out with SAINT [Siemens, 1995]. Absorption correction was performed by a multi-scan method implemented in SADABS [Bruker AXS Inc, 2014]. Crystal structures were solved using direct methods with SIR 2014 [Burla *et al.*,2015]. Structures were refined using the full-matrix least-squares method based on F^2 with SHELXL-2016 [Sheldrick, 2015]as implemented in the program suite WinGX/OLEX2 1.3 [Farrugia, 2012; Dolomanov *et al.*, 2009]. All non-hydrogen atoms were

refined anisotropically. Crystal data, data collection and structure refinement details are summarized in Table 1. All H atoms, apart from those on the N atom were positioned geometrically and refined using a riding model, with $U_{iso}(H) = 1.2U_{eq}(C)$. The H atom on the N atom was located in a difference Fourier map. The crystal structure of 4F has been transformed using suitable transformation matrix for the purpose of coherency in comparison of isostructural structures among Group 5. Crystal structure of 4F has been treated as two-component twin with the help of TWIN/BASF. The crystal packing and the structure overlay were generated using Mercury 4.2 [Macrae *et al.*, 2020]. Geometrical calculations were carried out using PARST [Nardelli, 1995] and PLATON [Spek, 2009].

S.3. Geometrical and Energetic parameters of interactions:

Crystal Packing Analysis: The crystal packing analysis has been performed after full convergence of refinement cycles using Mercury 4.2. The criteria for crystal packing analysis are sum of vdW radii of atoms involved + 0.2Å [Dance, 2003].

Total interaction energy using Crystal Explorer 17.5: In order to visualize the interaction topology in these crystal structures, energy framework analysis has been performed using CrystalExplorer 17.5. [Turner *et al.*, 2014; Mackenzie *et al.*, 2017]. The input file used for calculation is .cif. A 3.8Å cluster is drawn around the selected molecule and the incomplete molecules are completed. The interaction energy for unsubstituted, fluorine and chlorine substituted phosphoradimates are calculated by accurate energy model which includes B3LYP/6-31G (d, p) whereas B3LYP/DGDZVP have been employed for bromine and iodine substituted phosphoradimates. The calculation of the interaction energies is inclusive of normalization of C-H bond lengths to neutron distances. In this method, the values of interaction energies are used to construct the three-dimensional topology of interactions that are termed as energy frameworks. The pairwise intermolecular interaction energies in the crystal structures are represented as cylinders joining the molecules. The radii of these cylinders are proportional to the strength of the intermolecular interaction. The tube size was set at the default value of 80, with an energy cut-off of 4 kJ mol^{-1}. The values obtained from B3LYP/6-31G (d, p) are scaled for benchmarked energy models using k_ele=1.057, k_pol=0.740, k_disp=0.871, k_rep=0.618 [Turner *et al.*, 2017].

Xpac Analysis: All measurements were carried out using the *XPac 2.0* software using default values and filter settings of 10, 14, and 1.50, for the angular deviation (*a*), interplanar angular deviation (*p*), and corresponding molecular centroid distance deviation (*d*), respectively. [Gelbrich & Hursthouse, 2005; Gelbrich *et al.*, 2012] The result of *Xpac* analysis is tabulated in Table S8.

Table S2: Torsion angles (**τ1- τ6**) of unsubstituted and halogenated phosphoradimates

	2Cl	**Torsion angle (°)**	**2Br**	**Torsion angle (°)**	**2I**	**Torsion angle (°)**	**3Br**	**Torsion angle (°)**	**3I**	**Torsion angle (°)**
τ1	O3-P1-N1-C7	170.08(8)	O3-P1-N1-C7	170.81(12)	O3-P1-N1-C7	171.07(15)	O3-P1-N1-C7	179.93(15)	O3-P1-N1-C7	-179.0(2)
τ2	P1-N1-C7-C12	43.88(13)	P1-N1-C7-C12	43.0(2)	P1-N1-C7-C12	41.8(2)	P1-N1-C7-C12	5.4(3)	P1-N1-C7-C12	4.1(4)
τ3	O3-P1-O1-C1	-45.72(8)	O3-P1-O2-C13	-46.36(13)	O3-P1-O1-C1	-46.90(16)	O3-P1-O1-C1	-52.92(16)	O3-P1-O2-C13	-50.3(2)
τ4	P1-O1-C1-C2	-86.91(10)	P1-O2-C13-C18	-86.59(16)	P1-O1-C1-C6	-86.74(19)	P1-O1-C1-C2	-12.3(2)	P1-O2-C13-C14	-17.6(4)
τ5	O3-P1-O2-C13	63.48(9)	O3-P1-O1-C1	61.59(14)	O3-P1-O2-C13	61.16(16)	O3-P1-O2-C13	55.65(15)	O3-P1-O1-C1	56.3(2)
τ6	P1-O2-C13-C14	158.04(7)	P1-O1-C1-C6	158.99(11)	P1-O2-C13-C14	159.92(14)	P1-O2-C13-C18	91.54(18)	P1-O1-C1-C2	92.3(3)
	4Br	**Torsion angle (°)**	**4I**	**Torsion angle (°)**	**00**	**Torsion angle (°)**	**25F**	**Torsion angle (°)**	**3Cl**	**Torsion angle (°)**
τ1	O3-P1-N1-C7	171.11(17)	O3-P1-N1-C7	171.56(16)	O3-P1-N1-C13	178.86(12)	O3-P1-N1-C7	-177.24(16)	O3-P1-N1-C7	-178.8(2)
τ2	P1-N1-C7-C12	16.2(3)	P1-N1-C7-C8	13.6(3)	P1-N1-C13-C14	-4.3(2)	P1-N1-C7-C12	-11.6(3)	P1-N1-C7-C8	-0.4(4)
τ3	O3-P1-O2-C13	-49.51(18)	O3-P1-O2-C13	-49.98(16)	O3-P1-O2-C7	-51.28(13)	O3-P1-O2-C13	-41.16(15)	O3-P1-O1-C1	-67.2(2)

τ4	P1-O2-C13-C18	-87.4(2)	P1-O2-C13-C14	-89.96(19)	P1-O2-C7-C12	-170.52(10)	P1-O2-C13-C18	-83.35(19)	P1-O1-C1-C2	-158.9(2)
τ5	O3-P1-O1-C1	62.07(17)	O3-P1-O1-C1	61.97(15)	O3-P1-O1-C1	53.11(11)	O3-P1-O1-C1	68.30(16)	O3-P1-O2-C13	50.5(2)
τ6	P1-O1-C1-C2	118.60	P1-O1-C1-C6	116.61(17)	P1-O1-C1-C2	106.89(13)	P1-O1-C1-C2	159.85(13)	P1-O2-C13-C14	83.7(3)
	3F	**Torsion angle (°)**			**3F**	**Torsion angle (°)**				
τ1	O3-P1-N1-C7	179.8(4)		**τ1′**	O6-P2-N2-C25	-174.5(4)				
τ2	P1-N1-C7-C12	3.4(7)		**τ2′**	P2-N2-C25-C30	-14.1(7)				
τ3	O3-P1-O1-C1	-71.0(4)		**τ3′**	O6-P2-O5-C19	75.6(4)				
τ4	P1-O1-C1-C2	-149.3(4)		**τ4′**	P2-O5-C19-C24	149.6(4)				
τ5	O3-P1-O2-C13	51.9(4)		**τ5′**	O6-P2-O4-C31	-48.2(4)				
τ6	P1-O2-C13-C14	96.2(5)		**τ6′**	P2-O4-C31-C32	-103.9(5)				

τ1′-τ6′ refers to torsion angles for second molecule in the asymmetric unit.

S.3.1. 2Cl-2Br-2I

Table S3: Geometrical parameters and interaction energies of possible intra- and intermolecular interactions for 2Cl, 2Br and 2I respectively.

Motif No.	Interactions	Symmetry Code	D…A (Å)	H…A (Å)	D–H…A (°)	Energy (kJ/mol)
			2Cl			
0	C12-H12…O2	x, y, z	3.1859(14)	2.43	126	-
	C2-H2…C7	x, y, z	3.6261(14)	2.94	132	
	C18-H18…O3	x, y, z	3.2596(12)	2.55	122	
1	N1-H1…O3	-x, -y+2, -z+2	2.8748(10)	1.86	169	-84.4
	C18-H18…Cl1	-x, -y+2, -z+2	3.7410(12)	3.07	131	
	C17-H17…C3	-x, -y+2, -z+2	3.7982(15)	2.96	151	
	Cl1…O3	-x, -y+2, -z+2	3.3728(9)	-	140, 101	
II	C11-H11…O2	-x+1, -y+1, -z+2	3.2020(12)	2.70	108	-54.5
	C14-H14…O1	-x+1, -y+1, -z+2	3.6639(13)	2.74	143	
	C14-H14…C12	-x+1, -y+1, -z+2	3.8035(14)	3.05	139	
III	C3-H3…Cl1	-x, -y+2, -z+1	3.7740(11)	3.15	126	-11.4
	C4-H4…Cl1	-x, -y+2, -z+1	3.7295(12)	3.06	130	
IV	C15…C15	x, y-1, z+1	3.8545 (15)	-	-	-10.1
V	C7…C11	-x, -y+1, -z+2	3.4653(14)	-	-	-53.9
	C9-H9…C17	-x, -y+1, -z+2	3.5898(19)	2.87	135	
VI	C10-H10…C5	x, y-1, z	3.5301(15)	2.96	121	-19.2
			2Br			
0	C2-H2…O3	x, y, z	3.2561(19)	2.55	122	-
	C12-H12…O1	x, y, z	3.1682(22)	2.41	126	
	C18-H18…C7	x, y, z	3.6182(23)	2.93	132	

I	N1-H1…O3	-x, -y. -z+1	2.9051(16)	1.90	166	-90.8
	C2-H2…Br1	-x, -y. -z+1	3.7436(17)	3.11	127	
	Br1…O3	-x, -y. -z+1	3.4498(12)	-	138, 98	
	C3-H3…C17	-x, -y. -z+1	3.8227(22)	2.98	151	
II	C11-H11…O1	-x-1, -y+1, -z+1	3.2013(20)	2.68	109	-55.9
III	C16-H16…Br1	-x, -y, -z+2	3.7748(17)	3.10	131	-10.4
IV	C5…C5	-x-1, -y+1, -z	3.4494(27)	-	-	-12.0
V	C9-H9…C3	-x, -y+1, -z+1	3.5947(29)	2.85	166	-62.1
	C8…C12	-x, -y+1, -z+1	3.4122(22)	-	-	
VI	C10-H10…C14	x, y-1, z	3.5785(21)	2.95	126	-20.6
			2I			
0	C12-H12…O2	x, y, z	3.1513(1)	2.38	127	-
	C6-H6…C7	x, y, z	3.6099(2)	2.92	132	-
	C18-H18…O3	x, y, z	3.2635(2)	2.56	122	-
I	N1-H1…O3	-x+1, -y+1, -z+1	2.9051(16)	1.95	162	-89.5
	C18-H18…I1	-x, -y. -z+1	3.8089(3)	3.23	122	
	I1…O3	-x+1, -y+1, -z+1	3.5849(2)	-	137, 95	
II	C11-H11…O2/O1	-x+2, -y, -z+1	3.2318(2)	2.67	112	-51.7
III	C4-H4…I1	-x+1, -y+1, -z	3.8848(2)	3.20	133	-10.2
IV	C16-H16…C9	-x+1, -y, -z+1	3.8926(2)	3.20	168	-10.7
V	C9-H9…C17	-x+1, -y, -z+1	3.6276(2)	2.85	142	-66.2
	C8…C12	-x+1, -y, -z+1	3.4157(2)	-	-	
VI	C10-H10…C2	x, y-1, z	3.5484(2)	2.88	130	-19.2

a.

	N	Symop	R	Electron Density	E_ele	E_pol	E_dis	E_rep	E_tot
	0	-x, -y, -z	10.42	B3LYP/6-31G(d,p)	-5.5	-0.3	-16.1	14.2	-11.4
	0	-x, -y, -z	7.81	B3LYP/6-31G(d,p)	-4.7	-2.2	-32.5	14.2	-26.1
	1	-x, -y, -z	6.66	B3LYP/6-31G(d,p)	-18.7	-2.4	-82.6	64.1	-53.9
	1	-x, -y, -z	5.28	B3LYP/6-31G(d,p)	-78.7	-20.5	-52.0	96.0	-84.4
	0	x, y, z	11.10	B3LYP/6-31G(d,p)	-1.1	-0.4	-14.2	6.0	-10.2
	0	x, y, z	8.45	B3LYP/6-31G(d,p)	-0.4	-0.2	-9.2	4.7	-5.7
	2	x, y, z	9.22	B3LYP/6-31G(d,p)	-7.8	-3.4	-18.2	11.8	-19.2
	0	-x, -y, -z	5.59	B3LYP/6-31G(d,p)	-18.0	-4.3	-60.4	32.9	-54.5
	0	-x, -y, -z	11.47	B3LYP/6-31G(d,p)	-2.1	-0.8	-18.7	13.7	-10.6
	0	x, y, z	13.10	B3LYP/6-31G(d,p)	-2.2	-0.3	-11.0	9.5	-6.3
	0	-x, -y, -z	13.05	B3LYP/6-31G(d,p)	-4.5	-0.6	-13.4	11.1	-10.1

b.

	N	Symop	R	Electron Density	E_ele	E_pol	E_dis	E_rep	E_tot
	0	-x, -y, -z	9.97	B3LYP/DGDZVP	-8.8	-0.3	-18.9	22.8	-12.0
	1	-x, -y, -z	13.89	B3LYP/DGDZVP	-7.7	-0.7	-11.9	13.9	-10.4
	2	x, y, z	8.44	B3LYP/DGDZVP	-4.3	-0.3	-12.4	12.5	-7.9
	1	-x, -y, -z	6.27	B3LYP/DGDZVP	-43.0	-3.2	-89.2	102.6	-62.1
	1	x, y, z	9.21	B3LYP/DGDZVP	-12.0	-4.1	-19.0	18.9	-20.6
	0	x, y, z	13.18	B3LYP/DGDZVP	-2.1	-0.5	-9.9	8.7	-5.8
	1	-x, -y, -z	6.23	B3LYP/DGDZVP	-25.7	-5.0	-58.4	41.8	-55.9
	1	x, y, z	11.21	B3LYP/DGDZVP	-2.3	-0.5	-14.2	7.8	-10.4
	1	-x, -y, -z	5.16	B3LYP/DGDZVP	-90.8	-21.4	-56.2	113.3	-90.8
	1	-x, -y, -z	8.36	B3LYP/DGDZVP	-8.6	-2.4	-34.8	21.2	-28.1
	0	-x, -y, -z	11.42	B3LYP/DGDZVP	-8.3	-1.2	-18.7	24.2	-11.0

c.

	N	Symop	R	Electron Density	E_ele	E_pol	E_dis	E_rep	E_tot
	1	-x, -y, -z	5.21	B3LYP/DGDZVP	-87.9	-20.2	-60.2	114.6	-89.5
	0	x, y, z	8.48	B3LYP/DGDZVP	-8.9	-0.5	-16.1	22.0	-10.3
	0	-x, -y, -z	6.94	B3LYP/DGDZVP	-22.8	-4.6	-52.0	34.1	-51.7
	1	-x, -y, -z	6.02	B3LYP/DGDZVP	-45.5	-3.3	-95.2	108.9	-66.2
	2	x, y, z	9.28	B3LYP/DGDZVP	-11.7	-3.9	-18.8	19.1	-19.9
	0	x, y, z	13.34	B3LYP/DGDZVP	-1.0	-0.4	-7.9	5.4	-4.8
	0	x, y, z	11.42	B3LYP/DGDZVP	-2.5	-0.5	-13.9	7.0	-10.7
	0	-x, -y, -z	9.67	B3LYP/DGDZVP	-10.5	-0.3	-21.5	32.1	-10.2
	0	-x, -y, -z	8.91	B3LYP/DGDZVP	-8.8	-2.3	-36.4	24.2	-27.7
	0	-x, -y, -z	14.78	B3LYP/DGDZVP	-5.5	-0.6	-9.2	8.2	-9.2
	0	-x, -y, -z	11.47	B3LYP/DGDZVP	-8.4	-1.1	-17.7	23.6	-10.5

Fig S3: Total interaction energies decomposition into electrostatic, polarization, dispersion and repulsion components for **a.** 2Cl; **b.** 2Br; **c.** 2I.

S.3.2. 3Br-3I

Table S4: Geometrical parameters and interaction energies of possible intra- and intermolecular interactions for 3Br and 3I respectively.

Motif No.	**Interactions**	**Symmetry Code**	**D…A (Å)**	**H…A (Å)**	**D–H…A (°)**	**Energy (kJ/mol)**
			3Br			
0	C12-H12…O2	x, y, z	3.1692(20)	2.51	118	-
	C18-H18…C12	x, y, z	3.6408(34)	2.87	139	
1	N1-H1…O3	-x+2, -y+2, -z+1	2.8369(22)	1.84	163	-130.6
	C2-H2…O3	-x+2, -y+2, -z+1	3.4797(30)	2.42	168	
	C3-H3…C16	-x+2, -y+2, -z+1	3.867(34)	2.93	167	
II	Br1…O3	x+1, y+1, z	3.1101(14)	-	173, 100	-14.3
III	C16-H16…Br1	x+1, y, z	3.7971(29)	3.11	131	-14.3
IV	C4-H4…C9	x, y+1, z	3.5940(42)	2.66	167	-23.1
V	C5-H5…O2	-x+2, -y+2, -z	3.4211(27)	2.72	123	-35.3
	C6-H6…O2	-x+2, -y+2, -z	3.4216(28)	2.73	122	
	C6-H6…O1	-x+2, -y+2, -z	3.4078(26)	2.35	165	
VI	C11-H11…C15	-x+2, -y+1, -z	3.7669(28)	2.83	170	-27.0
			3I			
0	C12-H12…O1	x, y, z	3.1562(30)	2.50	118	
	C2-H2…C12	x, y, z	3.6105(53)	3.47	140	
I	N1-H1…O3	-x+2, -y+2, -z+1	2.8566(34)	1.86	162	-129.3
	C14-H14…O3	-x+2, -y+2, -z+1	3.5354(50)	2.46	172	
	C15-H15…C4	-x+2, -y+2, -z+1	3.8708(54)	2.94	168	

II	I1…O3	x+1, y+1, z	3.1715(22)	-	174, 101	-19.6
III	C4-H4…I1	x+1, y, z	3.9459(43)	3.25	132	-14.1
IV	C16-H16…C9	x, y+1, z	3.6255(63)	2.70	165	-22.1
V	C17-H17…O1	-x+2, -y+2, -z	3.4680(46)	2.74	125	-34.3
	C18-H18…O2	-x+2, -y+2, -z	3.4685(43)	2.81	121	
VI	C11-H11…C5	-x+2, -y+1, -z	3.7140(46)	2.78	169	-27.8

a.

	N	Symop	R	Electron Density	E_ele	E_pol	E_dis	E_rep	E_tot
	0	x, y, z	10.45	B3LYP/DGDZVP	-13.3	-1.8	-16.8	25.5	-14.3
	0	x, y, z	10.06	B3LYP/DGDZVP	-5.1	-1.1	-23.3	19.8	-14.3
	0	-x, -y, -z	6.56	B3LYP/DGDZVP	-21.1	-1.8	-49.5	50.3	-35.7
	1	-x, -y, -z	7.79	B3LYP/DGDZVP	-13.8	-2.0	-31.3	26.6	-27.0
	0	x, y, z	10.23	B3LYP/DGDZVP	-13.5	-1.6	-30.5	30.5	-23.1
	0	-x, -y, -z	9.10	B3LYP/DGDZVP	-2.8	-0.7	-10.8	7.5	-8.3
	1	-x, -y, -z	5.80	B3LYP/DGDZVP	-131.7	-32.7	-61.5	139.8	-130.6
	0	-x, -y, -z	9.02	B3LYP/DGDZVP	-1.4	-0.5	-13.3	7.9	-8.6
	1	-x, -y, -z	8.89	B3LYP/DGDZVP	-23.6	-3.3	-34.0	35.1	-35.3
	0	-x, -y, -z	11.75	B3LYP/DGDZVP	-16.4	-3.2	-16.7	15.9	-24.4

b.

	N	Symop	R	Electron Density	E_ele	E_pol	E_dis	E_rep	E_tot
	0	x, y, z	10.73	B3LYP/DGDZVP	-23.5	-2.6	-21.2	41.6	-19.6
	1	-x, -y, -z	6.36	B3LYP/DGDZVP	-125.2	-30.7	-58.9	124.9	-129.3
	0	-x, -y, -z	6.04	B3LYP/DGDZVP	-22.2	-1.7	-55.0	55.1	-38.6
	1	-x, -y, -z	8.15	B3LYP/DGDZVP	-15.5	-2.1	-33.7	31.7	-27.8
	0	-x, -y, -z	8.38	B3LYP/DGDZVP	-3.3	-1.0	-16.0	16.7	-7.9
	0	x, y, z	10.06	B3LYP/DGDZVP	-5.6	-1.1	-23.7	21.3	-14.1
	0	-x, -y, -z	8.87	B3LYP/DGDZVP	-4.1	-0.5	-15.9	16.6	-8.4
	0	x, y, z	10.46	B3LYP/DGDZVP	-11.8	-1.4	-28.7	26.7	-22.1
	1	-x, -y, -z	10.03	B3LYP/DGDZVP	-20.6	-3.1	-31.9	28.4	-34.3
	0	-x, -y, -z	12.49	B3LYP/DGDZVP	-15.3	-3.0	-16.2	14.7	-23.5

Fig S4: Total interaction energies decomposition into electrostatic, polarization, dispersion and repulsion components for a. 3Br; b. 3I.

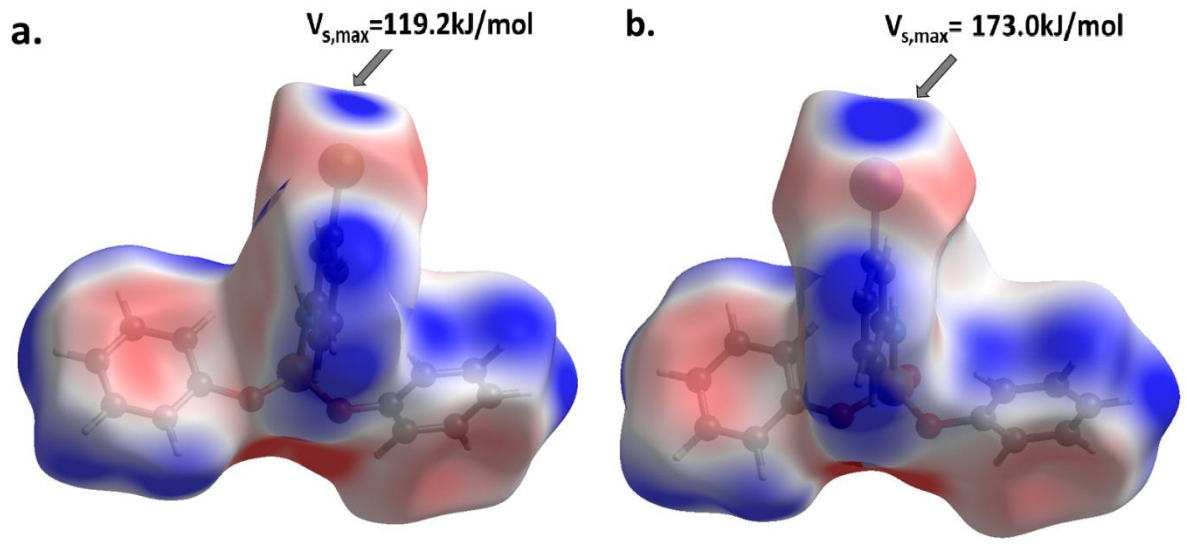

Fig S5: Electrostatic potential mapped over the Hirshfeld surface at a ±0.03 a.u. contour level showing σ-hole of **a.** bromine, **b.** iodine in 3Br and 3I respectively.

The molecular electrostatic surface potential has been mapped over the Hirshfeld Surface using Crystal Explorer 17.5. [Spackman *et al.*, 2008] For this purpose, *ab initio* wave functions were obtained at B3LYP/DGDZVP. The blue region depicts the electrostatic positive potential whereas the red region depicts the electrostatic negative potential. Here, the blue region shown in Fig S5 represents the σ-hole present in 3Br (a.) and 3I (b.). Clearly, the σ-hole for iodine has more negative potential with $V_{s,max}$= 173kJ/mol whereas bromine has $V_{s,max}$= 119.2kJ/mol.

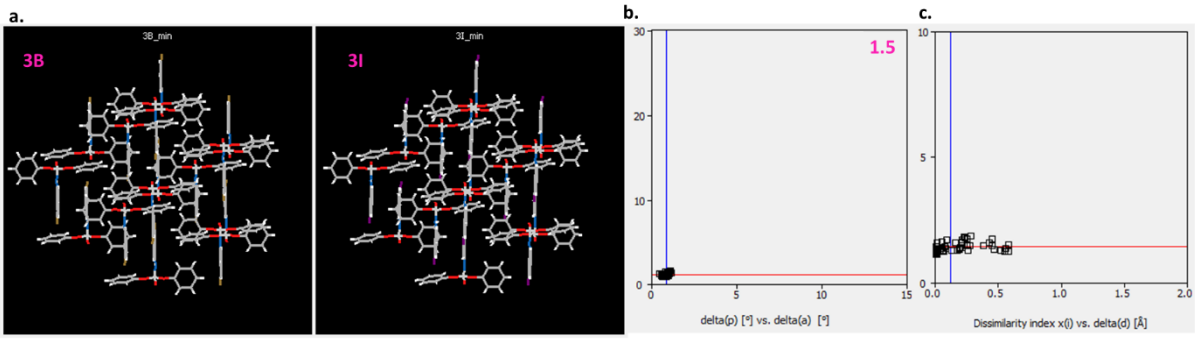

Fig S6: a. 3D supramolecular construct; **b.** Plot between delta[p] v/s delta[a] (with dissimilarity index mentioned in magenta at top right); **c.** Dissimilarity index (X) v/s delta[d] obtained from *Xpac* analysis for 3Br-3I.

S.3.3. 4Br-4I

Table S5: Geometrical parameters and interaction energies of possible intra- and intermolecular interactions for 4Br and 4I respectively.

Motif No.	Interactions	Symmetry Code	D…A (Å)	H…A (Å)	D–H…A (°)	Energy (kJ/mol)
			4Br			

0	C6-H6…O3	x, y, z	.	2.70	111	-
	C12-H12…O1	x, y, z	3.2590(27)	2.55	122	
	C12-H12…O2	x, y, z	3.2148(27)	2.70	109	
	C18-H18…C7	x, y, z	3.5774(28)	2.85	134	
1	N1-H1…O3	-x+1/2, y+1/2, -z+1/2	2.8124(23)	1.79	171	-63.8
	C8-H8…O3	-x+1/2, y+1/2, -z+1/2	3.4146(28)	2.63	129	
	C5-H5…C17	-x+1/2, y+1/2, -z+1/2	3.5454(36)	2.75	142	
	C14-H14…C6	-x+1/2, y+1/2, -z+1/2	3.8211(33)	2.95	153	
	C15-H15…C5	-x+1/2, y+1/2, -z+1/2	3.6148(35)	2.98	126	
II	C8-H8…O1	x, y+1, z	3.3271(25)	2.71	116	-23.8
	C8-H8…O2	x, y+1, z	3.3908(25)	2.68	123	
	C9-H9…O2	x, y+1, z	3.4107(27)	2.73	121	
III	C4-H4…C8	-x+1/2, -y+1/2, -z+1	3.6323(29)	2.75	154	-31.3
	C3…C3	-x+1/2, -y+1/2, -z+1	3.4887(38)	-	-	
IV	C2-H2…C15	x, -y, z-1/2	3.6496(38)	2.87	140	-17.9
V	Br1…C14	-x, y-1, -z+1/2	3.5221(24)	-	168	-8.1
VI	C11-H11…C18	-x, y, -z+1/2	3.8233(33)	2.96	152	-33.3
			4I			
0	C2-H2…O3	x, y, z	3.2500(24)	2.72	110	-
	C8-H8…O1	x, y, z	3.2716(24)	2.57	122	
	C8-H8…O2	x, y, z	3.2055(24)	2.67	110	
	C14-H14…C7	x, y, z	3.5934(25)	2.90	133	

I	N1-H1…O3	-x+3/2, y-1/2, -z+1/2	2.8037(20)	1.78	172	-65.1
	C12-H12…O3	-x+3/2, y-1/2, -z+1/2	3.3594(23)	2.56	131	
	C3-H3…C15	-x+3/2, y-1/2, -z+1/2	3.6011(32)	2.81	143	
	C18-H18…C2	-x+3/2, y-1/2, -z+1/2	3.8480(29)	2.90	153	
	C17-H17…C4	-x+3/2, y-1/2, -z+1/2	3.7405(33)	2.94	146	
II	C12-H12…O1	x, y+1, z	3.3591(22)	2.74	117	-23.7
	C11-H11…O2	x, y+1, z	3.4262(24)	2.74	122	
III	C4-H4…C11	-x+3/2, -y+1/2, -z	3.6524(27)	2.77	160	-31.3
IV	C6-H6…C17	x, -y, z+1/2	3.6935(34)	2.93	141	-17.7
V	I1…C13	-x+2, y+1, -z+1/2	3.6745(18)	-	150	-11.5
	I1…C18	-x+2, y+1, -z+1/2	3.5730(22)	-	167	
VI	C9-H9…C14	-x+2, y, -z+1/2	3.9636(29)	3.11	153	-34.2
	I1…C11	-x+2, y, -z+1/2	3.8763(18)	-	-	

a.

	N	Symop	R	Electron Density	E_ele	E_pol	E_dis	E_rep	E_tot
	1	-x+1/2, y+1/2, -z+1/2	7.62	B3LYP/DGDZVP	-62.7	-15.8	-47.6	90.2	-63.8
	1	x, y, z	7.27	B3LYP/DGDZVP	-9.2	-2.4	-24.5	14.6	-23.8
	1	-x+1/2, -y+1/2, -z	10.83	B3LYP/DGDZVP	-9.5	-1.2	-26.4	27.2	-17.1
	1	x, -y, z+1/2	10.28	B3LYP/DGDZVP	-7.4	-1.7	-20.8	15.0	-17.9
	1	-x+1/2, -y+1/2, -z	8.76	B3LYP/DGDZVP	-18.2	-1.7	-48.1	50.2	-31.3
	0	-x, y, -z+1/2	9.63	B3LYP/DGDZVP	-4.3	-0.3	-12.8	12.7	-8.1
	0	x, -y, z+1/2	10.87	B3LYP/DGDZVP	-2.6	-0.3	-7.0	4.9	-6.1
	0	-x, y, -z+1/2	6.32	B3LYP/DGDZVP	-17.7	-2.0	-46.4	44.1	-33.3
	0	-x, -y, -z	12.47	B3LYP/DGDZVP	-6.5	-0.6	-12.4	13.9	-9.5

b.

	N	Symop	R	Electron Density	E_ele	E_pol	E_dis	E_rep	E_tot
	1	-x, y, -z+1/2	9.38	B3LYP/DGDZVP	-9.9	-0.5	-18.3	24.7	-11.5
	1	-x+1/2, y+1/2, -z+1/2	8.43	B3LYP/DGDZVP	-64.5	-16.1	-47.9	91.8	-65.1
	0	-x+1/2, -y+1/2, -z	11.32	B3LYP/DGDZVP	-9.3	-1.2	-26.3	26.8	-17.0
	0	-x+1/2, -y+1/2, -z	8.92	B3LYP/DGDZVP	-18.5	-1.7	-47.0	49.4	-31.3
	0	x, -y, z+1/2	10.46	B3LYP/DGDZVP	-6.7	-1.6	-20.6	13.7	-17.7
	0	x, y, z	7.34	B3LYP/DGDZVP	-8.5	-2.2	-24.4	13.2	-23.7
	0	x, -y, z+1/2	10.70	B3LYP/DGDZVP	-3.7	-0.4	-8.1	8.0	-6.4
	1	-x, y, -z+1/2	5.83	B3LYP/DGDZVP	-20.7	-2.0	-50.1	53.0	-34.2
	0	-x, -y, -z	12.77	B3LYP/DGDZVP	-5.5	-0.5	-11.0	10.8	-9.1

Fig S7: Total interaction energies decomposition into electrostatic, polarization, dispersion and repulsion components for **a.** 4Br; **b.** 4I.

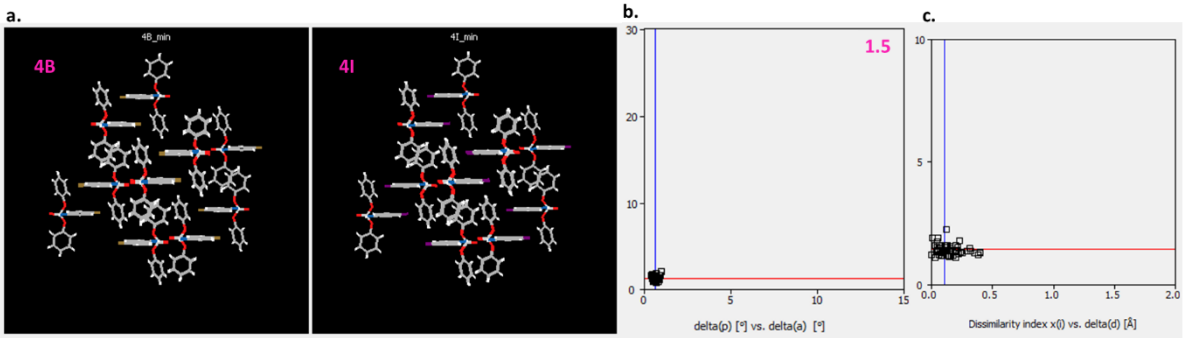

Fig S8: a. 3D supramolecular construct; **b.** Plot between delta[p] v/s delta[a] (with dissimilarity index mentioned in magenta at top right); **c.** Dissimilarity index (X) v/s delta[d] obtained from *Xpac* analysis for 4Br-4I.

S.3.4. 3F-34FN

Table S6: Geometrical parameters and interaction energies of possible intra- and intermolecular interactions for 3F.

Motif No.	**Interactions**	**Symmetry Code**	**D…A (Å)**	**H…A (Å)**	**D–H…A (°)**	**Energy (kJ/mol)**
			3F			
1	N1-H1N…O6	x, y, z	2.8047(55)	1.79	168	-66.2
	C8-H8…O6	x, y, z	3.3766(65)	2.56	132	
	C35-H35…C16	x, y, z	3.7244(89)	2.88	149	
II	N2-H2N…O3	x, y+1, z	2.8282(57)	1.82	165	-67.5
	C26-H26…O3	x, y+1, z	3.2982(65)	2.47	133	
	C18-H18…O6	x, y+1, z	3.3704(63)	2.39	151	
III	C8-H8…O2	x, y-1, z	3.3678(64)	2.49	138	-19.5
	C12-H12…F1	x, y-1, z	3.3354(62)	2.33	154	
	F1…O2	x, y+1, z	3.0726(49)	-	120, 106	
IV	C30-H30…F2	x, y-1, z	3.3503(62)	2.37	151	-21.8
V	C15-H15…C36	-x+1/2, y, z-1/2	3.8648(85)	2.91	178	-18.6
VI	C32-H32…C16	-x+1/2, y+1, z-1/2	3.5815(86)	2.84	136	-21.7
	C16-H16…C26	-x+1/2, y-1, z+1/2	3.7150(75)	2.78	170	
VII	C22-H22…C12	-x, -y+1, z-1/2	3.6882(76)	2.81	155	-27.0
	C22…C3	-x, -y+1, z-1/2	3.4433(88)	-	-	
VIII	C23…C2	-x, -y, z-1/2	3.5302(84)	-	-	-11.3
IX	F1…C29	x, y, z+1	3.2366(65)	-	-	-12.2
X	F2…C11	x, y-1, z+1	3.2482(60)	-	-	-12.5

	N	Symop	R	Electron Density	E_ele	E_pol	E_dis	E_rep	E_tot
	1	-	6.10	B3LYP/6-31G(d,p)	-53.8	-15.3	-48.6	71.8	-66.2
	1	-x, -y, z+1/2	11.47	B3LYP/6-31G(d,p)	-2.3	-0.4	-8.9	5.6	-7.0
	1	-	9.68	B3LYP/6-31G(d,p)	-9.6	-1.0	-33.2	29.2	-21.7
	1	x, y, z	7.33	B3LYP/6-31G(d,p)	-7.7	-1.8	-21.4	13.9	-19.5
	0	-x, -y, z+1/2	10.11	B3LYP/6-31G(d,p)	-1.6	-0.6	-12.9	6.6	-9.3
	1	-	9.13	B3LYP/6-31G(d,p)	-6.9	-1.2	-44.4	32.1	-27.0
	0	-	10.33	B3LYP/6-31G(d,p)	-4.4	-0.5	-13.1	8.4	-11.3
	0	-	8.95	B3LYP/6-31G(d,p)	-2.1	-0.6	-18.5	10.2	-12.5
	0	-	6.20	B3LYP/6-31G(d,p)	-54.6	-15.9	-47.6	70.2	-67.5
	0	-	9.01	B3LYP/6-31G(d,p)	-2.6	-0.5	-17.0	9.4	-12.2
	1	-	9.62	B3LYP/6-31G(d,p)	-5.5	-0.7	-23.7	13.5	-18.6
	0	-x, -y, z+1/2	11.90	B3LYP/6-31G(d,p)	-0.3	-0.2	-3.6	0.3	-3.4
	0	x, y, z	7.33	B3LYP/6-31G(d,p)	-8.0	-1.8	-22.3	12.1	-21.8
	0	-x+1/2, y, z+1/2	12.39	B3LYP/6-31G(d,p)	-1.7	-0.2	-6.5	1.6	-6.6
	0	-x+1/2, y, z+1/2	10.00	B3LYP/6-31G(d,p)	-1.2	-0.5	-11.8	5.2	-8.7

Fig S9: Total interaction energies decomposition into electrostatic, polarization, dispersion and repulsion components for 3F.

S.3.5. 4F-4Cl-24F-34FB

The original unit cell-dimensions of 4F (input unit cell shown below) were transformed via suitable transformation matrix which led to exchange in *a*- and *b*- axis for better visual comparison with the rest of the isostructural crystal structures in the group in Fig 11.

Input unit cell (Å/°): 9.1472(7), 10.1275(7), 17.8782(14), 89.827(3),86.227(3), 88.646(3)

Transformation matrix: $\begin{pmatrix} 0 & -1 & 0 \\ 1 & 0 & 0 \\ 0 & 0 & 1 \end{pmatrix}$

Transformed unit cell (Å/°): 10.1285(7), 9.1480(7), 17.8798(14), 86.225(3), 90.171(3), 91.354(3)

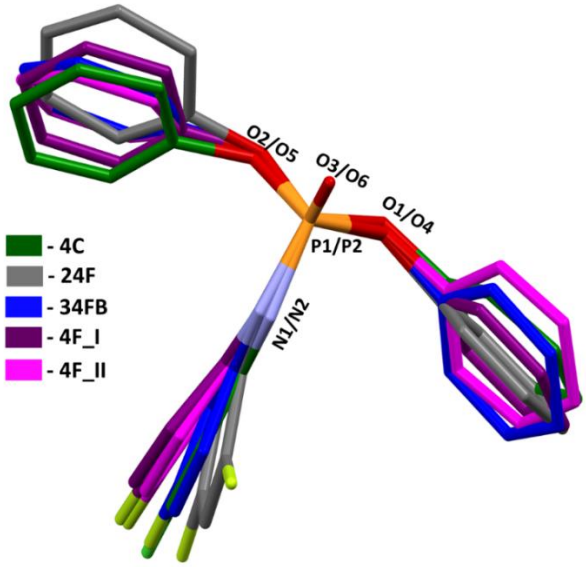

Fig S10: Molecular overlay of 4Cl, 24F, 34FB, 4F_I, 4F_II; Hydrogens have been removed for clarity.

Molecular overlay (Fig S10) has been performed with the help of Mercury 4.2 [Macrae *et al.*, 2020]. The molecules are superimposed keeping the orientation of the P=O bond fixed. This helps us in illustrating the deviation in conformation across -PO-/-PN- and -OPh/-NPh bonds. The RMS deviation for 4Cl-24F is 0.000909, 4Cl-34FB is 0.000209, 4Cl-4F_I is 0.000901 and 4Cl-4F_II is 0.000514.

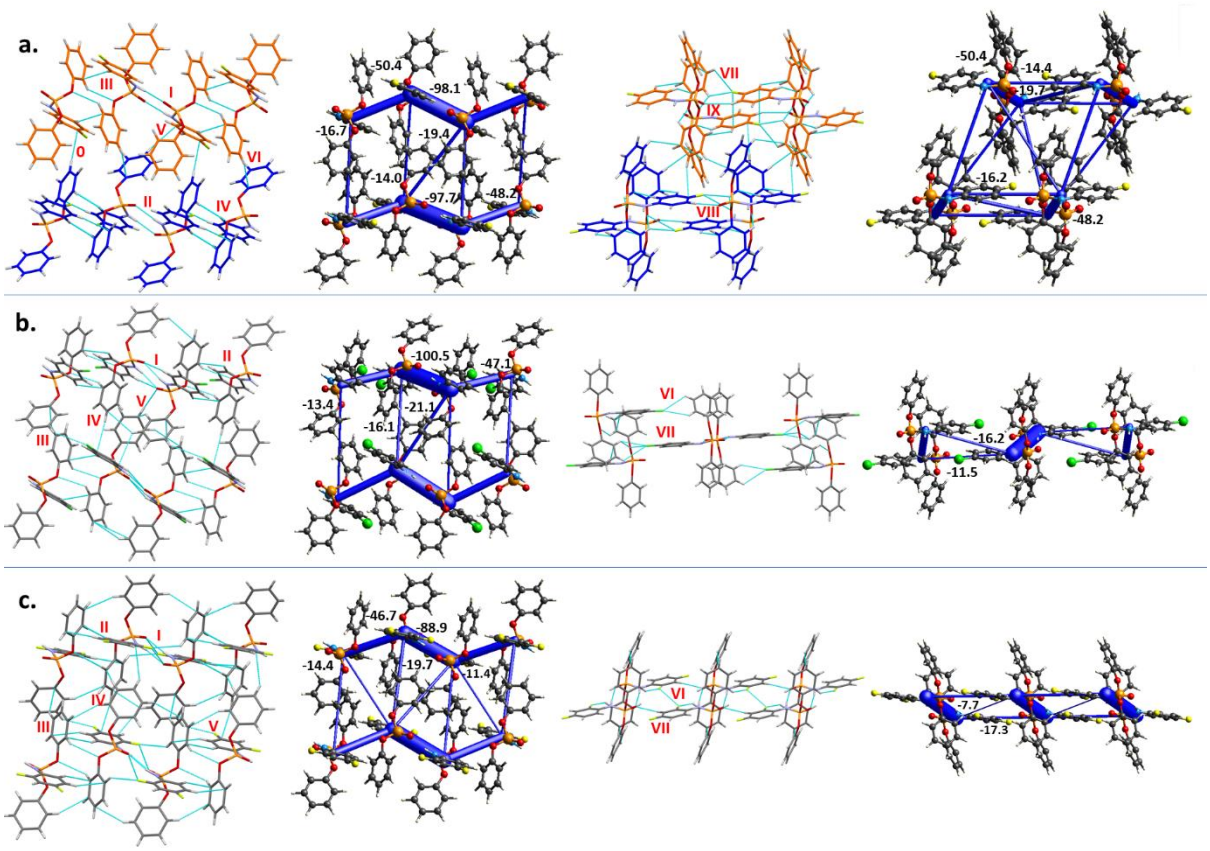

Fig S11: Crystalline arrangement for **a.** 4F (molecule 1 - orange, molecule 2 - blue); **b.** 4Cl; **c.** 24F along with their total interaction energies represented through energy frameworks respectively.

Table S7: Geometrical parameters and interaction energies of possible intra- and intermolecular interactions for 4F, 4Cl and 24F respectively.

Motif No.	**Interactions**	**Symmetry Code**	**D…A (Å)**	**H…A (Å)**	**D–H…A (°)**	**Energy (kJ/mol)**
			4F			
0	C22-H22…C16	x, y, z	3.6050(47)	2.68	165	-16.7
1	N1-H1…O3	-x+1,-y+1,-z	2.8109(32)	1.78	176	-98.1
	C18-H18…O3	-x+1,-y+1,-z	3.6399(35)	2.90	126	
	C9-H9…C4	-x+1,-y+1,-z	3.7457(58)	3.09	133	
II	N2-H2…O6	-x+1,-y+2,-z+1	2.8136(33)	1.79	174	-97.7
	C27-H27…C22	-x+1,-y+2,-z+1	3.7916(55)	2.85	133	
III	C24-H24…O4	-x+2,-y+2,-z+1	3.2514(35)	2.54	123	-50.4
	C30-H30…C22	-x+2,-y+2,-z+1	3.9546(56)	3.10	149	
	C35-H35…C20	-x+2,-y+2,-z+1	3.7828(47)	3.03	136	
IV	C2-H2A…O1	-x+2, -y+1, -z	3.2579(36)	2.66	114	-48.2
	C14-H14…C2	-x+2, -y+1, -z	3.8098(42)	2.89	163	
V	C21-H21…C7	x,+y+1,+z	3.6553(52)	2.82	148	-14.0
VI	C10-H10…C32	-x+1,-y+1,-z+1	3.6476(51)	2.98	128	-19.4
VII	C24-H24…F2	-x+2,-y+1,-z+1	3.2941(36)	2.53	127	-19.7
	C23-H23…F2	-x+2,-y+1,-z+1	3.3992(40)	2.76	117	
	F2…C35	-x+2,-y+1,-z+1	3.3588(39)	-	-	
VIII	C2-H2A…F1	-x+2,-y+2,-z	3.3160(36)	2.41	141	-16.2
IX	C33-H33…O6	x, y-1,+z	3.4889(37)	2.45	161	-14.4
			4Cl			

0	C2-H2…O3	x, y, z	3.2707(21)	2.58	121	-
	C12-H12…O1	x, y, z	3.1316(19)	2.44	121	
	C12-H12…O2	x, y, z	3.2141(19)	2.64	113	
I	N1-H1…O3	-x+1, -y+1, -z+1	2.8180(18)	1.80	172	-100.5
	C8-H8…O3	-x+1, -y+1, -z+1	3.5761(20)	2.81	128	
	C3-H3…C16	-x+1, -y+1, -z+1	3.6795(27)	3.04	126	
II	C14-H14…O2	-x+2, -y+1, -z+1	3.3632(20)	2.63	124	-47.1
	C12-H12…C14	-x+2, -y+1, -z+1	3.6159(23)	2.86	137	
III	C17-H17…C1	x, -y+3/2, z+1/2	3.6352(26)	2.76	153	-13.4
IV	C16-H16…C10	x, -y+1/2, z+1/2	3.7703(25)	2.82	174	-16.1
V	C4-H4…O3	-x+1, y-1/2, -z+3/2	3.7458(24)	2.88	138	-21.1
	C2-H2…C4	-x+1, y-1/2, -z+3/2	3.8410(28)	3.10	136	
VI	C15-H15…Cl1	-x+2, -y, -z+1	3.5323(20)	2.86	119	-16.2
	C14-H14…Cl1	-x+2, -y, -z+1	3.4906(17)	2.79	122	
VII	Cl1…O2	x, y-1, z	3.3682(12)	-	118, 108	-11.5
			24F			
0	C18-H18…O3	x, y, z	3.2715(28)	2.54	124	-
	C2-H2…O3	x, y, z	3.1310(28)	2.63	108	
	C12-H12…O1	x, y, z	3.2319(26)	2.50	124	
I	N1-H1…O3	-x, -y+1, -z+1	2.8597(22)	1.85	165	-88.9
	C2-H2…F1	-x, -y+1, -z+1	3.3965(26)	2.55	135	
	F1…O3	-x, -y+1, -z+1	3.1655(18)	-	146, 115	
	C17-H17…C4	-x, -y+1, -z+1	3.6535(35)	2.84	144	

II	C6-H6…O1	-x+1, -y+1, -z+1	3.2597(25)	2.67	114	-46.7
	C12-H12…C6	-x+1, -y+1, -z+1	3.7984(31)	2.89	159	
	C11-H11…C2	-x+1, -y+1, -z+1	3.7550(32)	2.99	138	
	C14-H14…C5	-x+1, -y+1, -z+1	3.8131(35)	2.95	151	
III	C3-H3…C13	x, -y+3/2, z-1/2	3.5820(32)	2.76	146	-14.4
IV	C4-H4…C10	x, -y+1/2, z-1/2	3.7490(33)	2.93	145	-19.7
	C15-H15…C6	x, -y+1/2, z+1/2	3.6067(33)	2.99	124	
V	C15-H15…F2	-x+1, y+1/2, -z+3/2	3.4796(28)	2.69	129	-11.4
VI	F1…F1	-x, -y, -z+1	2.7753(17)	-	99, 99	-7.7
VII	C9-H9…O3	x, y-1, z	3.4900(26)	2.46	160	-17.3
	C2-H2…C9	x, y-1, z	3.8512(31)	2.98	153	
	F2…O1	x, y-1, z	3.0825(19)	-	126, 101	

a.

N	Symop	R	Electron Density	E_ele	E_pol	E_dis	E_rep	E_tot
1	-x, -y, -z	5.61	B3LYP/6-31G(d,p)	-18.5	-4.4	-65.0	47.2	-50.4
1	-	9.25	B3LYP/6-31G(d,p)	-2.2	-0.8	-28.8	18.2	-16.7
1	-	9.77	B3LYP/6-31G(d,p)	-2.2	-0.3	-6.0	0.7	-7.2
1	-x, -y, -z	9.31	B3LYP/6-31G(d,p)	-4.6	-1.2	-24.5	12.1	-19.7
0	-	9.48	B3LYP/6-31G(d,p)	-3.6	-0.9	-29.5	21.2	-17.0
1	-	9.43	B3LYP/6-31G(d,p)	-2.2	-0.3	-5.8	0.5	-7.2
0	-	13.30	B3LYP/6-31G(d,p)	-0.4	-0.1	-2.8	0.2	-2.8
1	x, y, z	9.15	B3LYP/6-31G(d,p)	-6.0	-2.1	-15.0	10.7	-14.4
0	-x, -y, -z	5.84	B3LYP/6-31G(d,p)	-101.5	-24.4	-48.6	112.6	-98.1
0	-	9.37	B3LYP/6-31G(d,p)	-5.1	-1.3	-21.7	9.4	-19.4
0	-x, -y, -z	9.21	B3LYP/6-31G(d,p)	3.8	-0.7	-6.7	1.4	-1.5
0	-	9.94	B3LYP/6-31G(d,p)	-3.8	-1.0	-19.6	8.3	-16.6
0	-	12.72	B3LYP/6-31G(d,p)	-0.6	-0.1	-3.0	0.2	-3.2
0	-	10.57	B3LYP/6-31G(d,p)	-5.7	-0.8	-16.6	11.4	-14.0
1	-	11.36	B3LYP/6-31G(d,p)	-6.5	-0.7	-16.9	13.0	-14.0
0	-x, -y, -z	9.03	B3LYP/6-31G(d,p)	-6.1	-1.0	-23.6	14.2	-19.0
0	-x, -y, -z	5.91	B3LYP/6-31G(d,p)	-16.4	-4.0	-61.8	41.9	-48.2
0	-x, -y, -z	5.77	B3LYP/6-31G(d,p)	-100.1	-24.6	-46.7	108.5	-97.7
0	-x, -y, -z	9.19	B3LYP/6-31G(d,p)	4.1	-0.8	-7.5	2.0	-1.6
0	x, y, z	9.15	B3LYP/6-31G(d,p)	-8.5	-2.5	-17.7	16.4	-16.2

b.

N	Symop	R	Electron Density	E_ele	E_pol	E_dis	E_rep	E_tot
1	-x, -y, -z	9.25	B3LYP/6-31G(d,p)	-7.9	-1.2	-30.9	32.4	-16.2
1	-x, -y, -z	6.16	B3LYP/6-31G(d,p)	-101.6	-24.8	-51.6	113.8	-100.5
0	-x, -y, -z	6.10	B3LYP/6-31G(d,p)	-16.4	-3.5	-58.0	37.8	-47.1
0	x, -y+1/2, z+1/2	11.16	B3LYP/6-31G(d,p)	-6.0	-0.7	-16.1	12.0	-13.4
1	x, y, z	9.32	B3LYP/6-31G(d,p)	-2.2	-1.5	-15.6	9.1	-11.5
0	-x, y+1/2, -z+1/2	9.54	B3LYP/6-31G(d,p)	-6.0	-1.6	-23.4	11.0	-21.1
0	x, -y+1/2, z+1/2	9.28	B3LYP/6-31G(d,p)	-2.3	-1.0	-25.9	15.6	-16.1
0	-x, y+1/2, -z+1/2	9.38	B3LYP/6-31G(d,p)	-3.3	-0.3	-8.1	3.8	-8.5
0	-x, -y, -z	9.29	B3LYP/6-31G(d,p)	3.3	-0.5	-4.6	0.3	-0.7

c.

N	Symop	R	Electron Density	E_ele	E_pol	E_dis	E_rep	E_tot
0	x, y, z	9.34	B3LYP/6-31G(d,p)	-7.6	-2.1	-18.0	12.9	-17.3
0	x, -y+1/2, z+1/2	9.07	B3LYP/6-31G(d,p)	-1.4	-0.8	-32.8	17.7	-19.7
0	-x, -y, -z	8.74	B3LYP/6-31G(d,p)	-0.2	-0.2	-13.5	7.2	-7.7
0	-x, y+1/2, -z+1/2	9.56	B3LYP/6-31G(d,p)	-3.6	-1.6	-18.3	7.5	-16.3
0	-x, -y, -z	5.78	B3LYP/6-31G(d,p)	-81.3	-18.2	-55.6	95.3	-88.9
0	x, -y+1/2, z+1/2	11.25	B3LYP/6-31G(d,p)	-6.8	-0.8	-18.2	15.0	-14.4
0	-x, -y, -z	9.19	B3LYP/6-31G(d,p)	-3.2	-0.5	-15.3	3.9	-14.6
0	-x, y+1/2, -z+1/2	9.18	B3LYP/6-31G(d,p)	-3.6	-0.5	-10.9	3.8	-11.4
0	-x, -y, -z	6.44	B3LYP/6-31G(d,p)	-16.9	-3.9	-62.4	45.8	-46.7

Fig S12: Total interaction energies decomposition into electrostatic, polarization, dispersion and repulsion components for **a.** 4F; **b.** 4Cl and **c.** 24F respectively.

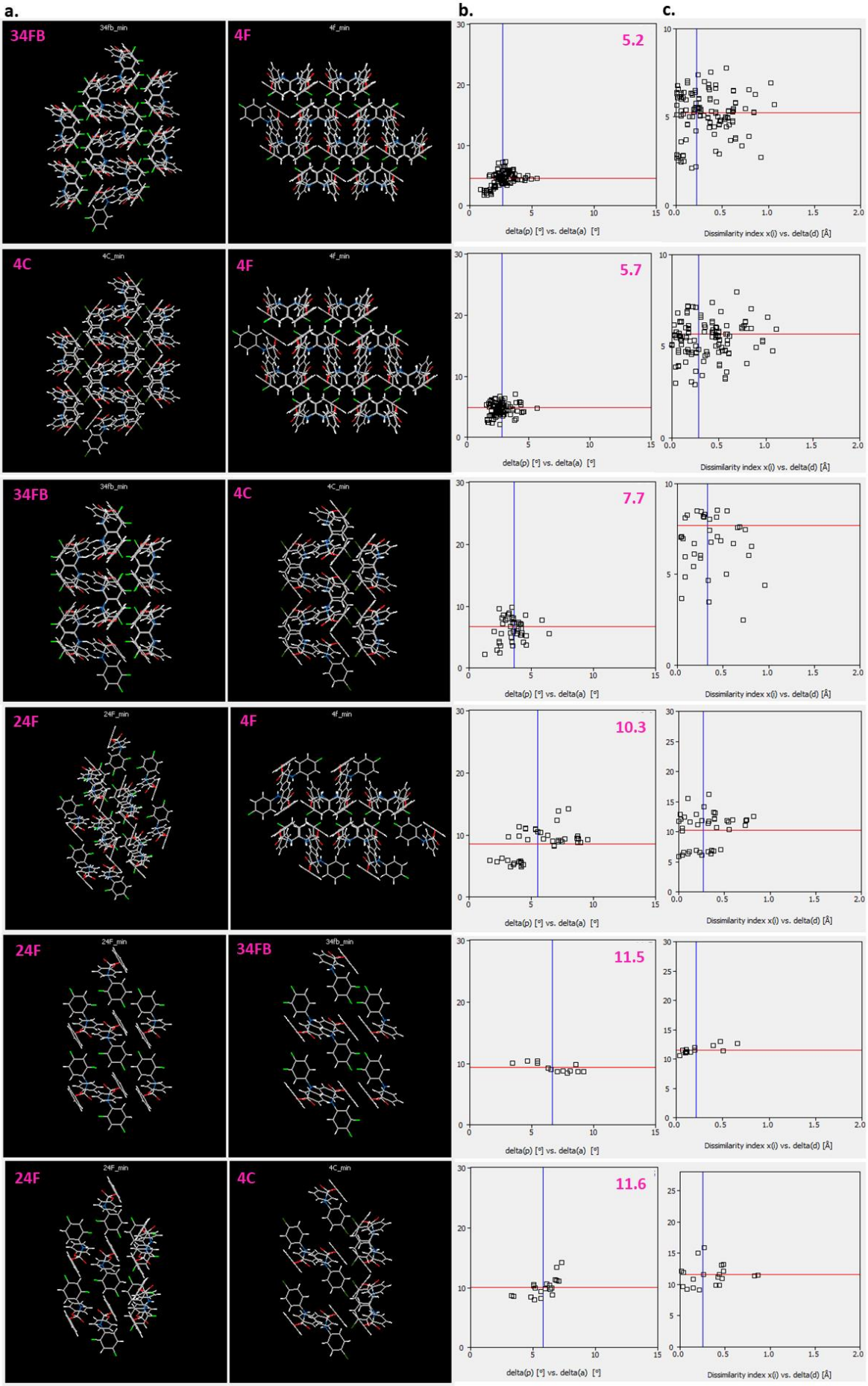
a.
b.
c.
34FB
34fb_min
4F
4f_min
5.2
4C
4c_min
5.7
7.7
24F
24f_min
10.3
11.5
11.6
delta(p) [°] vs. delta(a) [°]
Dissimilarity index x(i) vs. delta(d) [Å]

Fig S13: a. 3D supramolecular construct; **b.** Plot between delta[p] v/s delta[a]; **c.**Dissimilarity index (X) v/s delta[d] obtained from Xpac analysis for 34FB-4F, 4Cl-4F, 34FB-4Cl, 24F-4F, 24F-34FB and 24F-4Cl.

Table S8: Structural similarity (3D/1D) parameters for the isostructural halogenated phosphoradimates

S.No.	Compound code	Isostructurality	Dissimilarity Index (X)	Stretch Parameter (D/Å)	Δa (°)	Δp (°)
2Cl-2Br-2I						
1.	2Cl-2Br	3D	1.2	0.06	0.6	1.0
2.	2Br-2I	3D	2.0	0.12	0.9	1.8
3.	2Cl-2I	3D	3.1	0.18	1.4	2.8
3Br-3I						
1.	3Br-3I	3D	1.5	0.13	0.8	1.2
4Br-4I						
1.	4Br-4I	3D	1.5	0.11	0.7	1.3
3F-34FN						
1.	SC-A	1D	5.9	0.08	2.8	5.2
2.	SC-B	3D	2.4	0.12	1.1	2.2
4F-4Cl-24F-34FB						
1.	34FB-4F	3D	5.2	0.22	2.7	4.5
2.	4Cl-4F	3D	5.7	0.28	2.8	4.8
3.	34FB-4Cl	3D	7.7	0.33	3.6	6.7
4.	24F-4F	3D	10.3	0.27	5.5	8.5
5.	24F-34FB	3D	11.5	0.21	6.6	9.3
6.	24F-4Cl	3D	11.6	0.25	5.8	10.0

S.3.6. 00-25F-3Cl

Table S9: Geometrical parameters and interaction energies of possible intra- and intermolecular interactions for 00, 25F and 3Cl respectively.

Motif No.	Interactions	Symmetry Code	D…A (Å)	H…A (Å)	D–H…A (°)	Energy (kJ/mol)
			00			
0	C6-H6…O3	x, y, z	3.106	2.71	101	-
	C8-H8…O3	x, y, z	3.154	2.45	122	

	C14-H14…O2	x, y, z	3.215	2.56	119	
	C14-H14…O1	x, y, z	3.373	2.79	114	
1	N1-H1N…O3	-x, -y, -z+1	2.845	1.85	161	-99.9
	C18-H18…O3	-x, -y, -z+1	3.508	2.78	124	
	C9-H9…C4	-x, -y, -z+1	3.5717(23)	3.03	118	
II	C14-H14…C2	-x, -y+1, -z+1	3.7350(21)	2.92	145	-34.1
	C15-H15…C6	-x, -y+1, -z+1	3.6788(22)	2.83	150	
III	C4-H4…C17	x+1, y, z	3.7806(23)	2.89	157	-24.7
	C5-H5…C8	x-1, y, z	3.9540(20)	3.04	162	
IV	C9-H9…C17	-x+1, -y, -z+1	3.7469(22)	3.00	137	-13.5
V	C16-H16…O3	x+1/2, -y+1/2, z+1/2	3.3142(17)	2.42	140	-18.4
VI	C3-H3…C8	x+1/2, -y+1/2, z-1/2	3.9960(22)	3.09	159	-22.9
	C2-H2…C10	x+1/2, -y+1/2, z-1/2	3.0570(20)	2.86	127	
VII	C9…C12	-x+1/2, y-1/2, -z+1/2	3.7293(21)	-	-	-15.1
			25F			
0	N1-H1…F1	x, y, z	2.6822(23)	2.28	101	-
	C12-H12…O2	x, y, z	3.2022(21)	2.51	121	
I	N1-H1…O3	-x, -y, -z	2.8276(27)	1.83	162	-83.0
	C6-H6…C17	-x, -y, -z	3.6945(36)	3.07	125	
	C5-H5…C17	-x, -y, -z	3.6773(38)	3.02	128	
	F1…O3	-x, -y, -z	3.1419(16)	-	113, 145	
II	C12-H12…O1	-x, -y+1, -z	3.5573(30)	2.70	136	-49.1
	F2…O1	-x, -y+1, -z	3.1175(20)	-	111, 98	
	C14-H14…F2	-x, -y+1, -z	3.5388(28)	2.65	140	

	F2…O2	-x, -y+1, -z	3.1723(21)	-	111, 108	
	C2-H2…O2	-x, -y+1, -z	3.5802(23)	2.59	152	
	C2-H2…C13	-x, -y+1, -z	3.5004(28)	2.65	149	
III	C4-H4…F1	x+1, y, z	3.4323(25)	2.43	154	-21.6
	C18-H18…C3	x+1, y, z	3.7721(31)	2.94	147	
	C17-H17…C2	x+1, y, z	3.7429(29)	3.04	132	
IV	C17-H17…F2	-x-1, -y+1, -z	3.4005(25)	2.72	121	-21.1
	C16-H16…F2	-x-1, -y+1, -z	3.3998(26)	2.71	121	
V	C6…C5	-x+1, -y, -z	3.5923(25)	-	-	-19.9
VI	C9-H9…C2	-x, -y+1, -z-1	3.7964(31)	2.90	159	-41.2
	C10-H10…C5	-x, -y+1, -z-1	3.6844(28)	2.92	138	
	C8…C10	-x, -y+1, -z-1	3.3744(29)	-	-	
			3Cl			
0	C8-H8…O1	x, y, z	3.2047(33)	2.60	115	-
	C8-H8…O2	x, y, z	3.2452(33)	2.62	116	
	C6-H6…O3	x, y, z	3.3354(33)	2.64	122	
I	N1-H1…O3	-x+1, -y, -z+1	2.8367(34)	1.84	163	-103.6
	C12-H12…O3	-x+1, -y, -z+1	3.4795(31)	2.75	125	
	C5-H5…C16	-x+1, -y, -z+1	3.7547(56)	3.05	132	
II	C2-H2…O2	-x+1, -y, -z	3.5727(37)	2.53	162	-43.7
	C18-H18…Cl1	-x+1, -y, -z	3.9143(34)	3.13	142	
	Cl1…O2	-x+1, -y, -z	3.4600(22)	-	112, 103	
III	C4-H4…O3	x-1/2, -y+1/2, z-1/2	3.5779(36)	2.60	150	-13.0
IV	C17-H17…C3	-x+3/2, y-1/2, -z+1/2	3.6597(50)	2.90	137	-8.6
V	C5…C11	-x+1/2, y-1/2, -z+1/2	3.5478(40)	-	-	-16.8
VI	C15-H15…C10	x+1/2, -y-1/2, z+1/2	3.7856(48)	2.88	160	-11.1

VII	C11-H11…C2	-x, -y, -z	3.6462(41)	2.92	134	-46.3
	C9…C11	-x, -y, -z	3.3590(41)	-	-	

a.

N	Symop	R	Electron Density	E_ele	E_pol	E_dis	E_rep	E_tot
1	-x, -y, -z	5.16	B3LYP/6-31G(d,p)	-88.1	-23.4	-63.3	106.2	-99.9
0	x, y, z	9.82	B3LYP/6-31G(d,p)	-9.7	-1.2	-34.2	26.2	-24.7
0	-x, -y, -z	12.93	B3LYP/6-31G(d,p)	-1.5	-0.1	-3.3	0.3	-4.4
1	-x+1/2, y+1/2, -z+1/2	9.47	B3LYP/6-31G(d,p)	-5.1	-1.2	-12.9	4.0	-15.1
0	-x, -y, -z	5.83	B3LYP/6-31G(d,p)	-9.7	-1.9	-49.7	33.9	-34.1
1	x+1/2, -y+1/2, z+1/2	9.87	B3LYP/6-31G(d,p)	-8.2	-1.3	-32.1	23.6	-22.9
1	x+1/2, -y+1/2, z+1/2	9.14	B3LYP/6-31G(d,p)	-9.2	-2.5	-18.8	15.5	-18.4
0	-x, -y, -z	8.88	B3LYP/6-31G(d,p)	-2.0	-0.6	-20.1	10.8	-13.5
0	-x+1/2, y+1/2, -z+1/2	10.35	B3LYP/6-31G(d,p)	-1.0	-0.3	-8.2	3.2	-6.4
0	-x, -y, -z	9.29	B3LYP/6-31G(d,p)	-2.8	-0.5	-19.6	11.7	-13.2

b.

N	Symop	R	Electron Density	E_ele	E_pol	E_dis	E_rep	E_tot
0	-x, -y, -z	4.84	B3LYP/6-31G(d,p)	-15.5	-3.0	-72.2	52.5	-49.1
1	x, y, z	9.22	B3LYP/6-31G(d,p)	-6.6	-1.0	-28.8	18.1	-21.6
1	-x, -y, -z	5.69	B3LYP/6-31G(d,p)	-71.3	-18.7	-54.2	86.6	-83.0
1	x, y, z	11.26	B3LYP/6-31G(d,p)	-2.6	-0.5	-7.3	2.9	-7.7
1	-x, -y, -z	11.06	B3LYP/6-31G(d,p)	-4.4	-1.2	-9.8	2.8	-12.3
1	-x, -y, -z	15.00	B3LYP/6-31G(d,p)	-0.7	-0.3	-5.8	4.7	-3.0
1	-x, -y, -z	7.79	B3LYP/6-31G(d,p)	-15.0	-2.3	-61.9	48.8	-41.2
1	x, y, z	10.04	B3LYP/6-31G(d,p)	-2.0	-0.2	-9.0	3.6	-7.9
1	-x, -y, -z	8.89	B3LYP/6-31G(d,p)	-4.7	-0.8	-27.8	14.1	-21.1
1	x, y, z	13.01	B3LYP/6-31G(d,p)	-0.0	-0.2	-7.6	3.3	-4.7
1	x, y, z	11.04	B3LYP/6-31G(d,p)	-0.6	-0.2	-2.5	0.3	-2.8
1	-x, -y, -z	9.12	B3LYP/6-31G(d,p)	-3.7	-3.9	-24.3	13.1	-19.9

c.

N	Symop	R	Electron Density	E_ele	E_pol	E_dis	E_rep	E_tot
1	-x, -y, -z	6.12	B3LYP/6-31G(d,p)	-97.0	-26.3	-53.1	104.7	-103.6
1	x+1/2, -y+1/2, z+1/2	10.49	B3LYP/6-31G(d,p)	-2.8	-0.7	-17.7	12.5	-11.1
1	-x, -y, -z	7.45	B3LYP/6-31G(d,p)	-15.3	-2.2	-69.0	51.3	-46.3
1	x, y, z	11.37	B3LYP/6-31G(d,p)	0.0	-0.3	-6.1	4.1	-3.0
1	x, y, z	9.67	B3LYP/6-31G(d,p)	-1.1	-0.6	-10.7	5.5	-7.6
1	x+1/2, -y+1/2, z+1/2	10.93	B3LYP/6-31G(d,p)	-5.1	-2.1	-11.2	5.7	-13.0
2	-x+1/2, y+1/2, -z+1/2	9.82	B3LYP/6-31G(d,p)	-3.4	-0.7	-23.7	12.8	-16.8
1	-x, -y, -z	4.65	B3LYP/6-31G(d,p)	-17.4	-3.1	-67.6	58.2	-43.7
0	-x+1/2, y+1/2, -z+1/2	12.27	B3LYP/6-31G(d,p)	-0.8	-0.1	-2.2	0.2	-2.6
0	-x+1/2, y+1/2, -z+1/2	11.05	B3LYP/6-31G(d,p)	-1.4	-0.6	-13.3	7.9	-8.6
0	-x, -y, -z	11.07	B3LYP/6-31G(d,p)	-3.6	-0.8	-4.3	0.1	-8.0

Fig S14: Total interaction energies decomposition into electrostatic, polarization, dispersion and repulsion components for **a.** 00; **b.** 25F and **c.** 3Cl respectively.

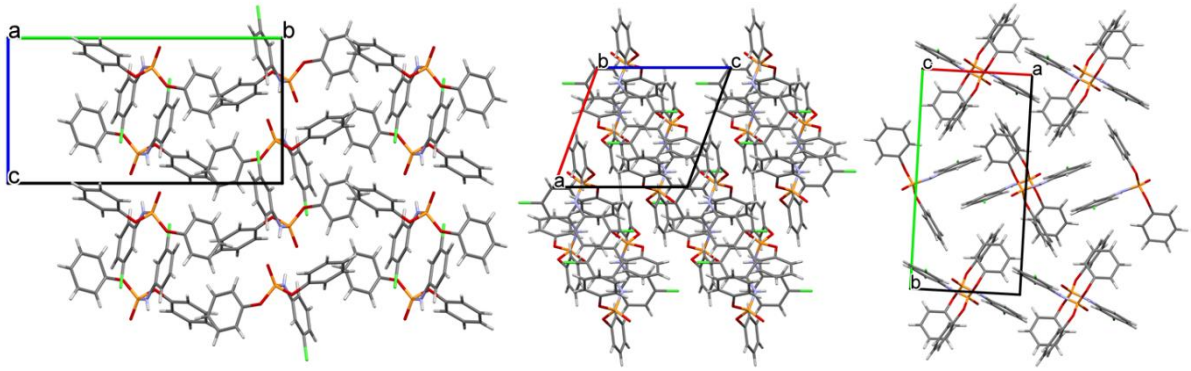

Fig S15: The arrangment of molecules in crystal of 3Cl, down the a-, b- and c-axis respectively (left to right).

S.4. Hirshfeld surface analysis and Fingerprint plots

With the help of 'Hirshfeld surface generation' option in Crystal Explorer 17.5., a surface was generated for molecule in asymmetric unit for unsubstituted and halogenated phosphoradimates. Based on the surface generated, the % contribution of contacts is extracted using Finger print plot (shown below Fig S16).

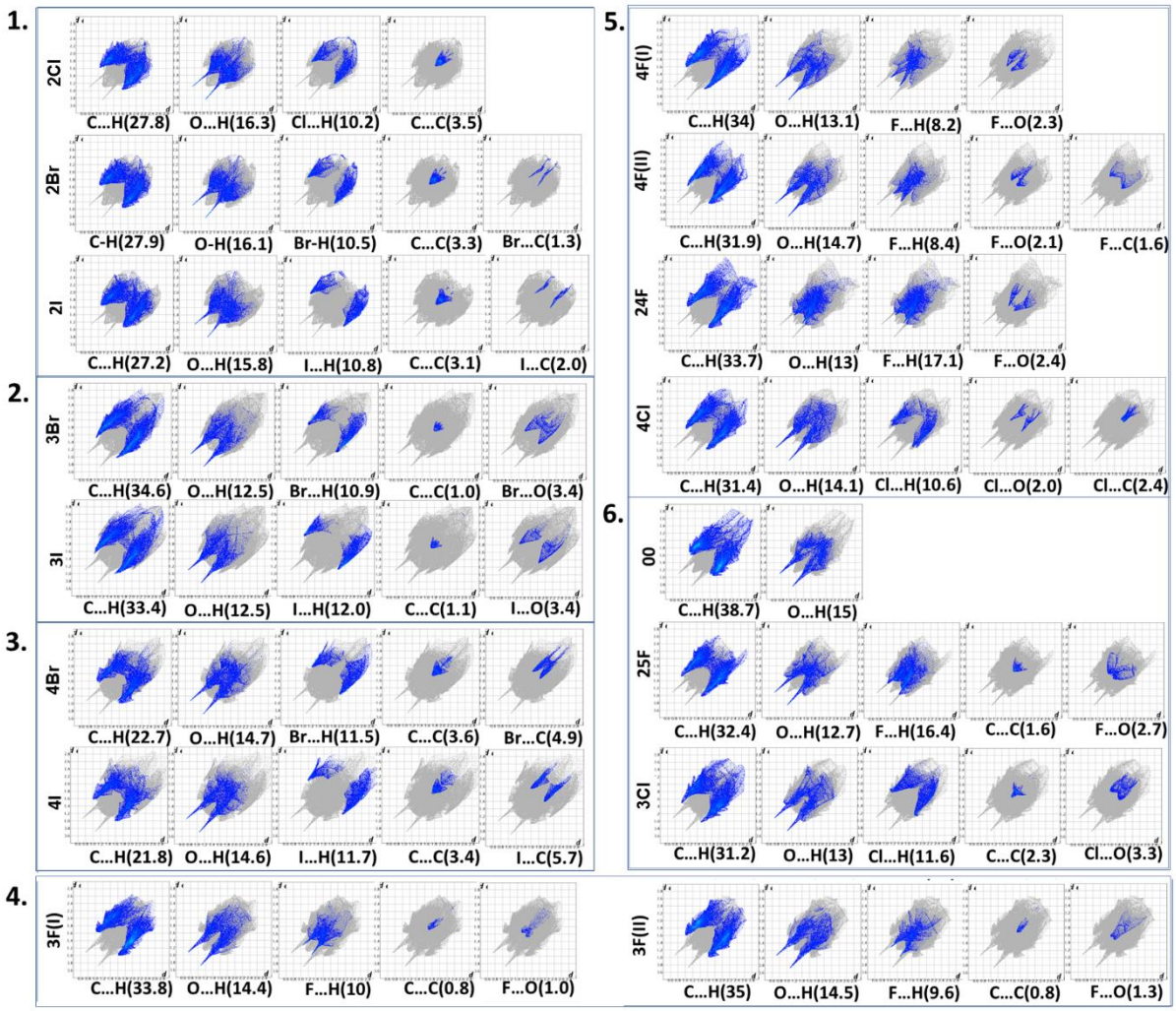

Fig S16: Fingerprint plots of **1.** 2Cl-2Br-2I, **2.** 3Br-3I, **3.** 4Br-4I, **4.** 3F (I, II), **5.** 4F (I, II)-24F-4C, **6.** 00-25F-3Cl depicting % contribution of C···H/H···C, O···H/H···O, H···X/X…H, C…C, X…C/C…X, X···O/O…X and other contacts. (X= F/Cl/Br/I). The value in the bracket represents their contribution percentage.

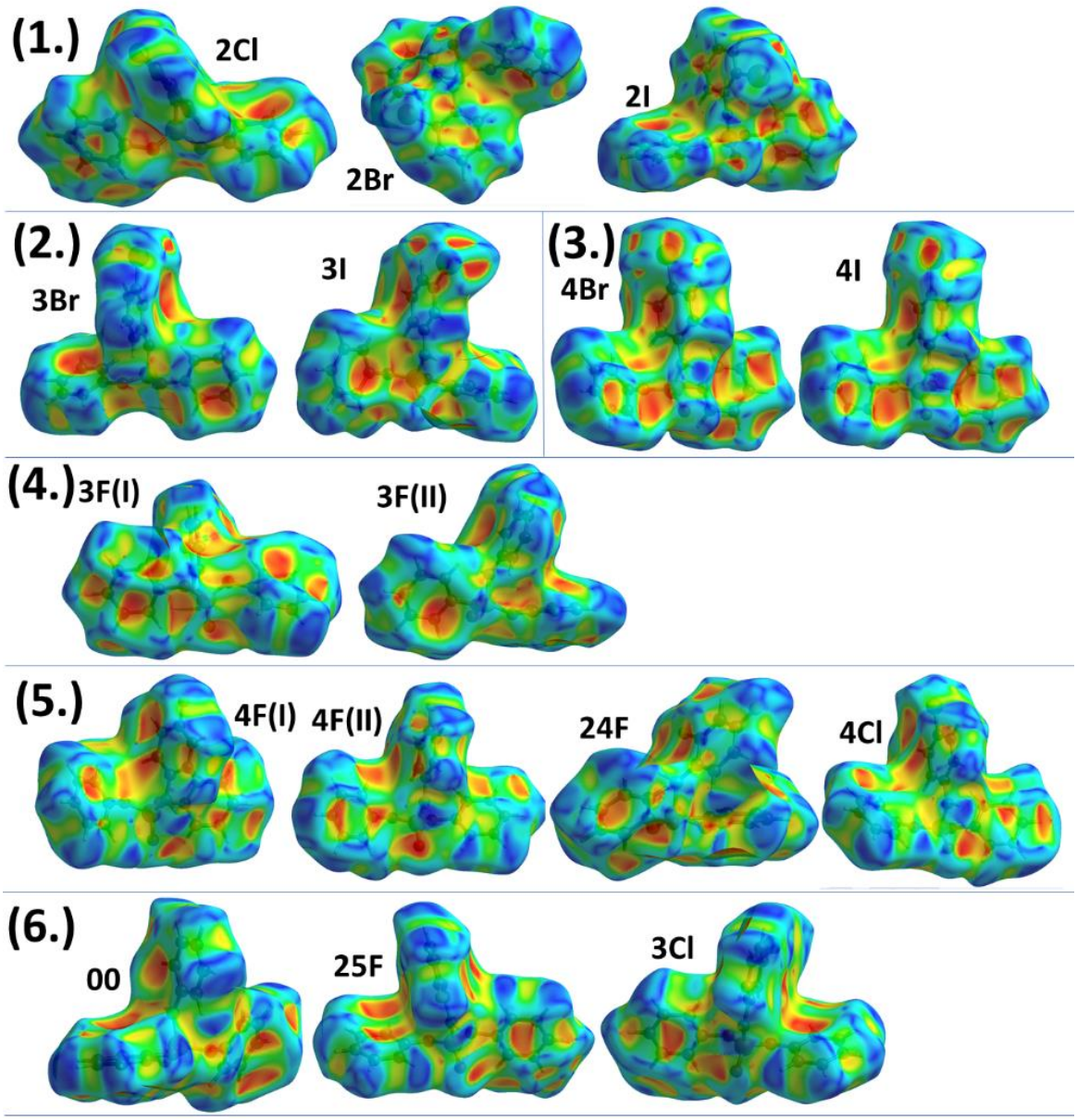

Fig S17: Shape index of **1.** 2Cl-2Br-2I, **2.** 3Br-3I, **3.** 4Br-4I, **4.** 3F (I, II), **5.** 4F (I, II)-24F-4C, **6.** 00-25F-3Cl depicting the significant C-H…π interaction contribution by bright orange spot on the surface.

S.5. Square synthons

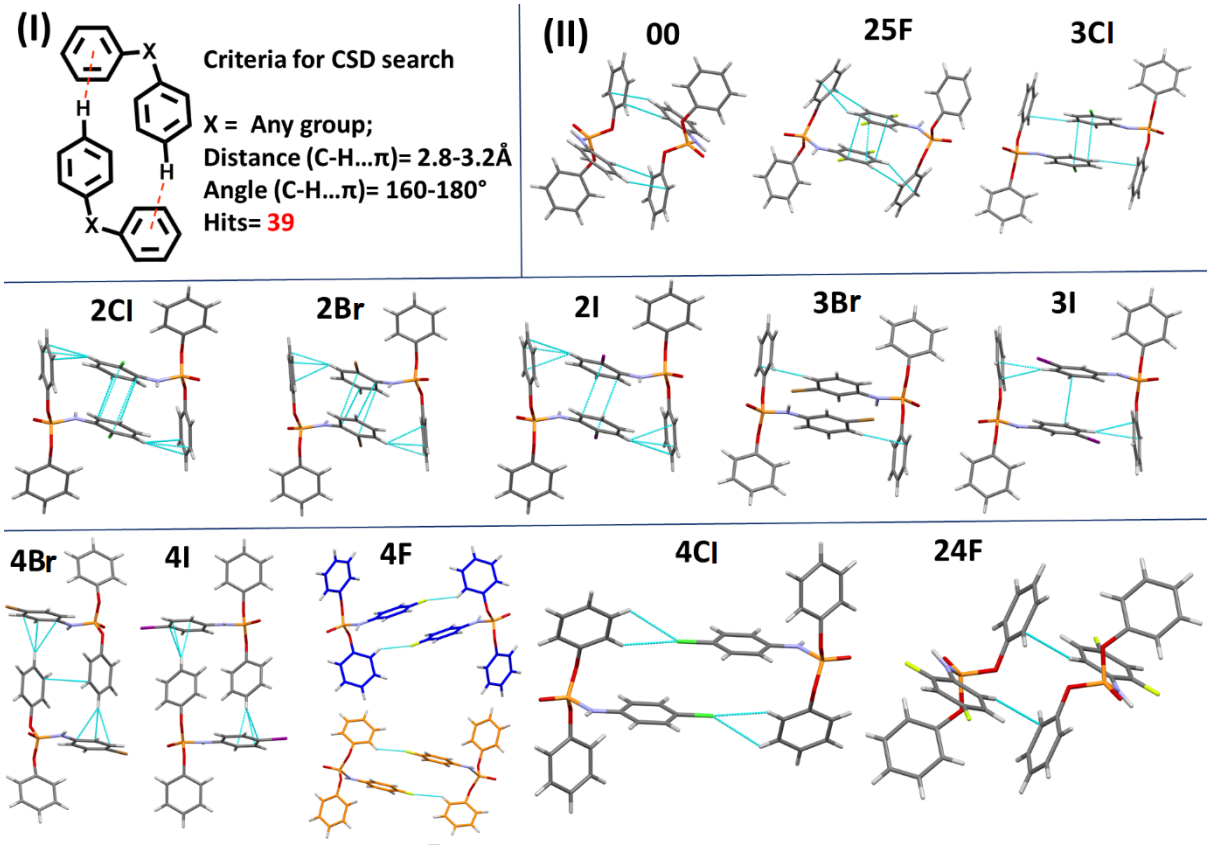

Fig S18: (I) Supramolecular square synthon searched in CSD database with search criteria; (II) Representation of square motifs present in unsubstituted and halogenated phosphoradimates.

S.6. Lattice Energy

Computation of Lattice energy using PixelC: The total interaction energy is the combination of coulombic, polarization, dispersion and repulsion contributions. The electron densities are calculated at the MP2/6-31G (d,p) level for unsubstituted, fluorine-, chlorine- and bromine-substituted phosphoradimates and at the MP2/DGDZVP level for iodine-substituted phosphoradimates using *GAUSSIAN09* [Frisch *et al.*, 2009]. The MLC files, which are generated after calculation, provide the computed values of lattice energies (Table 3 in the main article).

Computation of Lattice energy using Crystal Explorer 17.5: The lattice energy of unsubstituted and halogenated phosphoradimates are computed with the help of Crystal Explorer 17.5. For one molecule in the asymmetric unit, a cluster of 20Å is created around the selected molecule and the molecule fragments are completed. Further, the energy is computed for the cluster with the help of accurate method constituting of B3LYP/6-31G (d, p) for unsubstituted, fluoro and chloro substituted phosphoradimate, whereas, B3LYP/DGDZVP was used for bromo and iodo-substituted phosphoradimates. The energy is calculated by summing half of the product of N and E_{tot}. For $Z'>1$ molecule in the asymmetric unit, a cluster of 20Å is created around the selected molecule and the molecule fragments are completed. An average of the value obtained for the individual molecule selected is tabulated in Table 3 in the main article.

References:

Burla, M. C., Caliandro, R., Carrozzini, B., Cascarano, G. L., Cuocci, C., Giacovazzo, C., Mallamo, M., Mazzone, A. & Polidori, G. (2015). *J. Appl. Crystallogr.***48,** 306-309.

Dance, I. (2003) *New J. Chem.***, 27**, 22-27.

Dolomanov, O.V., Bourhis, L.J., Gildea, R.J, Howard, J.A.K. & Puschmann, H. (2009) *J. Appl. Cryst.*, **42**, 339-341.

Farrugia, L. (2012) *J. Appl. Crystallogr*., **45**, 849-854.

Frisch, M. J. *et al.* (2009). *Gaussian 09*, Revision A.02, Gaussian, Inc., Wallingford, CT, USA.

Gates-Rector, S. & Blanton, T. T. (2019) *Powder Diffr*., **34**, 4, 352–360.

Gelbrich, T. & Hursthouse, M. B. (2005) *CrystEngComm*, **7**, 324.

Gelbrich, T., Threlfall, T. L. & Hursthouse, M. B. (2012) *CrystEngComm*, **14**, 5454-5464.

Mackenzie, C.F., Spackman, P. R., Jayatilaka, D. & Spackman, M. A. (2017). *IUCrJ*, **4**, 575–587.

Macrae, C. F., Sovago, I., Cottrell, S. J., Galek, P. T. A., McCabe, P., Pidcock, E., Platings, M., Shields, G. P., Stevens, J. S., Towler, M. & Wood, P. A. (2020). *J. Appl. Cryst.* **53**, 226–235.

Nardelli, M., (1995). *J. Appl. Cryst.* **28**, 659.

SADABS (2014) Bruker AXS Inc., Madison, WI.

Sheldrick, G. (2015) *Acta Crystallogr. C***71**, 3-8.

Siemens, S. S. (1995) Siemens Analytical X-ray Instruments Inc. Madison, MI.

Spackman, M. A., McKinnon, J. J., Jayatilaka, D. (2008) *CrystEngComm*, **10**, 377– 388.

Spek, A. (2009) *Acta Crystallogr. D***65**, 148-155.

Turner, M. J., Grabowsky, S., Jayatilaka, D. & Spackman, M. A. (2014) *J. Phys. Chem. Lett*., **5**, 4249.

V. U. M. Apex2, (2006) Bruker Analytical X-ray Systems Madison, WI.